Delivering Strong ^{1}H Nuclei Hyperpolarization Levels and Long Magnetic Lifetimes through Signal Amplification by Reversible Exchange

Peter J. Rayner, Michael J. Burns, Alexandra M. Olaru, Philip Norcott, Marianna Fekete, Gary G. R. Green, Louise A. R. Highton, Ryan. E. Mewis and Simon. B. Duckett*

Centre for Hyperpolarisation in Magnetic Resonance, Department of Chemistry, University of York, Heslington, YO10 5NY

Hyperpolarization turns typically weak NMR and MRI responses into strong signals so that ordinarily impractical measurements become possible. The potential to revolutionize analytical NMR and clinical diagnosis through this approach reflect this area's most compelling outcomes. Methods to optimize the low cost *para*hydrogen based signal amplification by reversible exchange (SABRE) approach through studies on a series of biologically relevant nicotinamides and methyl nicotinates are first detailed. These procedures involve specific ^{2}H-labelling in both the agent and catalyst and achieve polarization lifetimes of *ca*. 2 minutes with 50% detectability in the case of 4,6-d_2-nicotinate. As a 1.5 T hospital scanner has an effective ^{1}H detectability level of just 0.0005% this strategy should result in compressed detection times for chemically discerning measurements that probe disease. To demonstrate this techniques generality, we exemplify further studies on a range of pyridazine, pyrimidine, pyrazine and isonicotinamide analogues that feature as building blocks in biochemistry and many disease treating drugs.

Hyperpolarization | SABRE | Catalysis | NMR | MRI

Introduction

By harnessing the magnetic properties of nuclei, we unlock nuclear magnetic resonance (NMR), one of the most powerful methods available for studying materials, which in the form of magnetic resonance imaging (MRI) revolutionizes clinical diagnosis.(1) One simple route to improve the diagnostic capabilities of MRI involves monitoring *in vivo* changes in metabolite flux in conjunction with spatially resolved measurements to non-invasively probe human physiology.(2) However, for reasons of low sensitivity, agent detection needs to be coupled with approaches to increase detectability.(3) This process is exemplified by studies on pyruvate which harnesses dissolution dynamic nuclear polarization (DNP)(4) to produce the signal strength necessary to track its metabolism. Additionally, the related method of optical pumping noble gases, such as ^{129}Xe,(5) has provided the sensitivity needed to produce lung MR images that probe pulmonary disease.

Both of these agents magnetic resonance (MR) detectability was greatly increased through a process known as hyperpolarization. However, the associated hyperpolarization step could be viewed as being complex.(6, 7) One related method of great promise is that of MR enhancement by *para*hydrogen (p-H_2).(8, 9) p-H_2 is a unique hyperpolarized feedstock which has no magnetic moment and is not observed itself.(10) Instead, a highly visible agent is obtained when it adds to an unsaturated center as a consequence of this chemical change.(10) The resulting products' intrinsic magnetization, more commonly referred to as polarization, can lie so far from thermodynamic equilibrium that measurements which normally take months become possible in seconds.(11) However, this is only possible if the agent's high-sensitivity monitoring takes place before relaxation returns its polarization to the more usual weak-signal level. Moreover, the associated magnetization can be examined just once at high sensitivity because the hyperpolarization process takes place outside the final readout-area. Hence the imaging of such agents after dosing in a clinical setting must be very rapid if the strong response is to survive the time taken to travel to this location. The development of this technique is, therefore fraught with experimental challenge as fresh samples are needed for each study. Furthermore, the use of NMR spectroscopy as an analytical tool would also benefit substantially if the materials it analyses can be rapidly characterized at lower concentrations than is currently possible.(12-14) Hence, harnessing the fruits of hyperpolarization will provide opportunities to improve our ability to study materials in a very wide range of applications.

Significance

The study of molecules and materials is of great significance to both science and human life, with non-invasive techniques such as nuclear magnetic resonance and magnetic resonance imaging reflecting some of the most important methods for probing them. However, both of these approaches are inherently insensitive and would benefit greatly from improved signal strengths. A strategy to optimize the Signal Amplification by Reversible Exchange (SABRE) is presented here that can improve signal strengths by over 100,000 times those which would be seen on a routine clinical MRI scanner after just 10 seconds of exposure to *para*hydrogen. Furthermore, by revealing the broad scope of this approach we demonstrate its potential for the future diagnostic detection of materials, metabolites or drugs by NMR or MRI.

In this study, we illustrate a number of new developments to dramatically improve the p-H_2 based method Signal Amplification By Reversible Exchange (SABRE).(15) This route shows great promise for contributing significantly to both analytical NMR and clinical diagnosis in the future.(16-21) SABRE does not change the chemical identity of the agent it hyperpolarizes, it simply equilibrates polarization between p-H_2 and the selected agent to create highly visible signals through earlier binding to a metal center.(15) This simple and cheap to implement process is shown schematically in Fig. 1 with the reproducible response being created in just a few seconds.(22) Furthermore, as it maintains its hyperpolarization while in the presence of p-H_2 it can maintain its polarization level for many

minutes in low field as it can be continually replenished (22, 23). Consequently we predict that the future *in vivo* optimization of this method will be easier than that of many other approaches if we can deliver agents with high signal strengths and appropriately long-lived magnetization.

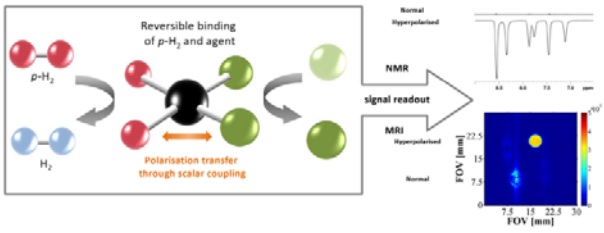

Fig. 1. Schematic representation of the SABRE effect

We present here a general strategy to achieve this aim by combining a series of breakthroughs in substrate and catalyst design. We illustrate this strategy through studies on nicotinamide (**1**) and methyl nicotinate (**2**), and a series of their selectively deuterated analogues, before demonstrating the approaches wider applicability. These two agents exhibit low toxicity and play important roles in cellular biology and hence are biochemically important targets.(24) The relaxation times and hyperpolarization levels of these biocompatible agents are shown to be dramatically increased by the selective use of spin-dilution through appropriate ^{2}H-labelling, a strategy that has already be deployed for DNP.(25) We overcome the fact that the SABRE catalyst ultimately reduces the levels of hyperpolarization through transfer to H_2 when *p*-H_2 is a limiting reagent(26) by improving on the lifetime of the agents' magnetization when bound to the catalyst through ^{2}H-labelling of its ancillary ligands. Subsequently, we show that by combining these strategic advances 50% hyperpolarization can be achieved in conjunction with magnetic-state lifetimes that approach 100 seconds for a ^{2}H-labelled nicotinate. By expanding the scope of this strategy to other target agents we show that a universal improvement in ^{1}H hyperpolarization level and relaxation time is achieved. The single-scan MRI detection of these agents is then used to reveal that these improvements facilitate the acquisition of images whose intensity and contrast are vastly superior to those without hyperpolarization. Whilst the relaxation times of these agents are reduced in H_2O solution, they still exhibit high detectability when compared to the results of normal study. Hence we are confident that the results presented here reflect a series of key steps towards successful *in vivo* SABRE whilst also serving to improve its potential as analytical tool for NMR.

Results and discussion

The SABRE method starts by dissolving an agent (substrate) in a solvent that contains a metal based polarization transfer catalyst and then exposing it to *p*-H_2 for a few seconds in low magnetic field. The hyperpolarized agent can then be detected in a second step by NMR or MRI methods. Protio-nicotinamide (**1**) was one of the first substrates to be polarized by SABRE(15) and aspects of its ^{1}H, ^{13}C and ^{15}N signal enhancement have been previously communicated.(27-31). When **1** is hyperpolarized in this way through SABRE(28) in methanol-d_4 solution, as detailed in the supporting information, the signal for H-2 is ca. 650 times larger than that observed in a control measurement under Boltzmann conditions at a 9.4 T field. In contrast, the corresponding signals for H-4, H-5 and H-6 are 620, 190 and 590 times larger respectively than those of the H-2 control signal. Fig. 2-left illustrates a typical measurement. This signal intensity corresponds to detecting 2.1% H-2 polarization, created after a combination of just 7 seconds exposure to 3 bar of *p*-H_2 and three seconds for subsequent transfer into the measurement field. The corresponding polarization values in ethanol-d_6 range from 1.1 to 0.1% as detailed in Table 1. It is therefore straightforward to conclude that **1** is highly amenable to SABRE. Furthermore, according to the laws of signal averaging, if 31 seconds were needed to repeat each control measurement, it would take *ca*. 150 days of data collection to reproduce the previously detailed hyperpolarized result if a normal signal were to be employed. It is for this reason that hyperpolarization represents a platform that could radically transform clinical diagnosis and analytical NMR more generally.

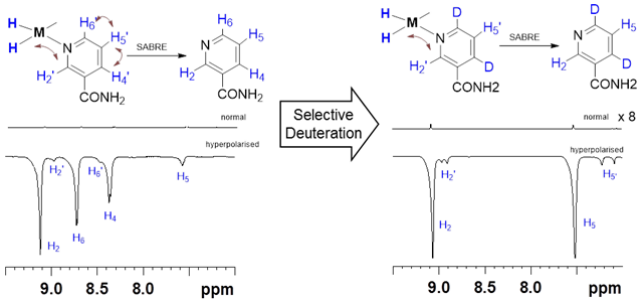

Fig. 2. SABRE hyperpolarization of nicotinamide: Left: Single scan ^{1}H NMR traces, with identical scaling, that illustrate nicotinamide (**1**) signals (as labelled) that result after SABRE (hyperpolarized) and when the polarization level matches that for thermodynamic equilibrium (normal). Right: Similar single scan ^{1}H NMR traces employing **1e** (Table 1); the normal trace has a x8 vertical expansion relative to the hyperpolarized trace (all measurements were performed in ethanol-d_6).

As we have indicated though, this signal gain must survive to the point of measurement. In methanol-d_4 solution, the four distinct protons resonances of **1**, H-2, H-4, H-5 and H-6, have T_1 values of 16.3, 11.3, 6.9 and 9.8 seconds at 9.4 T respectively (see Table 1, errors are <5% unless specified). These T_1 values change to 23.3 (50% increase), 6.7 (40% fall), 3.9 (45% fall) and 7.8 (20% fall) seconds respectively in ethanol-d_6 solution, and range from 10.7 to 6.5 seconds in D_2O solution. Hence these values are highly solvent dependent and not, at first glance, likely to be ideal for *in vivo* imaging; due to low SABRE efficiency in neat D_2O solutions the corresponding polarization levels are not reported.(32, 33)

Relaxation during SABRE catalysis

Examination of these NMR relaxation properties under SABRE conditions reveals that the observed T_1 values for the four proton signals of **1** reduce to just 6.2, 6.3, 3.7 and 3.8 seconds respectively in methanol-d_4. Furthermore, the H-2 T_1 value in ethanol-d_6 falls by 83% to 4.2 seconds thereby implying even faster signal destruction. These changes are explained by the role the SABRE catalyst plays in facilitating the reversible flow of polarization according to Fig. 1. During SABRE, rapid polarization transfer is beneficial, in leading to a large signal gain but at high field, or without *p*-H_2, the catalyst clearly destroys the contrast agents' hyperpolarization by reducing T_1.

Using ^{2}H-labelling to reduce agent relaxation

Initially, we proposed to overcome these effects by using ^{2}H-labelling to extend the proton relaxation times of **1**.(27) Hence,

nicotinamide derivatives **1a-1g** were prepared using the methods described in Fig. 3. These synthetic routes have been scaled to provide over 25 grams of the desired isotopologue and thus provide a robust platform to underpin any potential clinical/pre-clinical studies. Table 1 presents their SABRE performance and proton T_1 values, both with and without catalyst, at 9.4 T in methanol-d_4, ethanol-d_6 and D_2O solutions and clearly there is a beneficial extension in T_1.

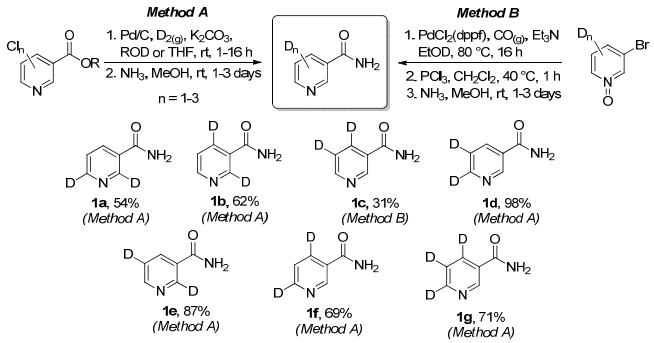

Fig. 3. Synthetic methods used to prepare agents **1a**-**1g**. Yields are isolated yields after column chromatography.

As these structures all contain fewer protons than **1**, they might be expected to achieve higher polarization levels under conditions when *p*-H_2 is the limiting reagent. However, substrate **1a**, whose *ortho* protons have been removed, gives low polarization under SABRE conditions. We conclude, therefore, that **1a** has polarization acceptor sites that are too magnetically isolated from the hydride ligands of the catalyst for effective SABRE transfer. In contrast, forms **1b-1g** all possess a proton adjacent to nitrogen, and based on the recent study by Tessari et al., the relative position of the *ortho* proton to the ring substituent is unlikely to affect its coupling with the hydride ligand in the catalyst.(34) They should therefore all receive polarization at a similar rate and hence the poor performance of **1c** under SABRE must be a consequence of rapid relaxation. Agents **1e** and **1f** have the largest average T_1 values of the series and perform best under SABRE. **1e** possesses a ^{4}J coupling between protons H-4 and H-6 that facilitates magnetization transfer between them and gives hyperpolarization levels of 2.7 and 3.2% respectively in methanol-d_4 (Fig. 1). For **1f**, the corresponding weaker ^{5}J coupling between protons H-2 and H-5 now results in 4.1% hyperpolarization levels. **1d**, with a ^{4}J, and **1b** with a ^{3}J coupling, and triply ^{2}H-labelled **1g** also perform less well than **1e** and **1f** which can readily be explained by their poor T_1 values. Hence we conclude that locating one proton next to the N-binding site (for strong coupling to the hydride ligands) and a longer-range coupling to a second longer-lived storage site is optimal.

Optimizing the SABRE catalysis of methyl nicotinate

As the amide protons of nicotinamide are likely to play a role in these relaxation processes the series of related methyl nicotinates **2a-2e**, shown in Table 2, were prepared and studied. The parent, protio-nicotinate **2**, proved to be superior to **1** under SABRE catalysis, with its four aromatic proton resonances showing an average polarization level of 2.7% in methanol-d_4 and 1.7% in ethanol-d_6 under our test; transfer to the methyl group is negligible. Furthermore, proton H-2 now has a T_1 value of 60 seconds in methanol-d_4, 49 seconds in ethanol-d_6 and 13.8 seconds in D_2O. In contrast, doubly ^{2}H-labelled 4,6-d_2-nicotinate (**2b**) has proton T_1 values in the absence of the catalyst for H-2 of 66 seconds and H-5 of 97.6 seconds in methanol-d_4. These drop to 46.2 and 62.7 seconds respectively in ethanol-d_6, but retain impressive values of 30.9 and 47.4 seconds in D_2O. As a consequence of these changes we boost the delivered SABRE polarization levels to 10.1% and 9.5% respectively in methanol whilst retaining an average hyperpolarization level of ca. 8.75% in ethanol-d_6. It proved possible to improve on these already impressive results by introducing a CD_3 label such that d_3-methyl 4,6-d_2-nicotinate (**2c**) exhibits T_1 values of 50.1 and 50.3 seconds in D_2O whilst achieving 7.2% polarization in ethanol-d_6.

Improving the SABRE catalyst through ^{2}H-labelling

The presence of the catalyst acts to reduce the measured T_1 values of the protons of the free substrate because the bound and free forms of the substrate are in dynamic exchange and consequently the recorded protons' T_1 values must reflect their appropriately weighted average. Hence, the T_1 value of a bound proton must be much smaller than the real value of the free material. We proved this by measuring the bound and free protons relaxation times at 263 K where ligand exchange is effectively quenched (see supporting information). We hypothesized that the slow rate of productive polarization transfer(15) means that any increase in the bound protons' relaxation times would be seen in an improved final agent polarization level. Conceptually, this could also be achieved by introducing ^{2}H-labelling into the N-heterocyclic carbene (NHC) ligand of the catalyst. Thus, we developed synthetic routes (see supporting information) to produce d_2-, d_{22}- and d_{24}-IMes ligands which were used to form the corresponding [IrCl(COD)(NHC)] catalyst (Fig. 4). The measured T_1 values of the protons in **2b** (bound and free) with these catalyst isotopomers, under 3 bar of H_2 or D_2, in methanol-d_4 solution are detailed in Table 3.

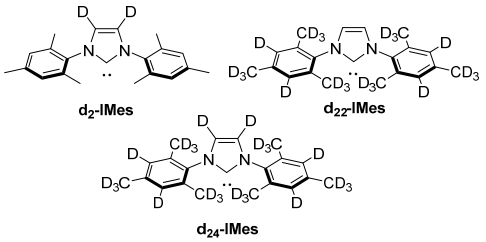

Fig. 4: ^{2}H-Labelled NHC ligands used for SABRE polarization with catalysts of type [IrCl(COD)(NHC)]

These data show that as predicted the T_1 values of the H-2 resonance in equatorially bound **2b** is increased by 36% on moving from H_2 to D_2 respectively at 263 K. This confirms that coupling to the hydride ligands provide a significant route to relaxation. Furthermore, on comparing the d_2-, d_{22}- and d_{24}-IMes systems, there is an increase in both the bound T_1 and free substrate T_1 values. More importantly, when moving to 298 K where SABRE catalysis is conducted,(35) further increases in the free substrates' protons T_1 values are observed. Consequently we re-examined the SABRE efficiency of **2b** with these catalysts (Table 4). Both the effective T_1 relaxation times and polarization levels increased with the best performing catalyst, [IrCl(COD)(d_{22}-IMes)] giving average polarization levels of ca. 22.0% under 3 bar *p*-H_2 in both methanol-d_4 and ethanol-d_6 which reflects a stunning 250% improvement in the latter case.

Up to this point we have conducted all SABRE catalysts under 3 bar pressure of *p*-H_2, which in our standard 5 mm J. Young's Tap NMR tubes reflects *ca.* 13-fold excess with respect to the substrate. Thus, if *p*-H_2 is the limiting reagent in this catalytic

process, the reaction will ultimately progress to a point where normal H_2 (formed by conversion of *p*-H_2) is the dominant form in solution. Hence the SABRE hyperpolarization of **2b** was re-examined with [IrCl(COD)(d_{22}-IMes)] in methanol-d_4 and ethanol-d_6 solution under 3.0-5.5 bar of *p*-H_2 (Fig. 5). In methanol-d_4 solution we see an increase in H-2 polarization to 26.4% and 28.5% at 4.0 and 5.5 bar respectively. A more dramatic effect is observed in ethanol-d_6 solution where a 55% increase in enhancement is observed at 5.5 bar of *p*-H_2 when compared to 3.0 bar. This results in a 41.7% polarization being measured on the H-2 site of **2b** under these conditions. These conditions are not used in the routine experiments we have described as they take the sample close to its safe pressure limit, and we would encourage any one repeating this work to take appropriate precautions.

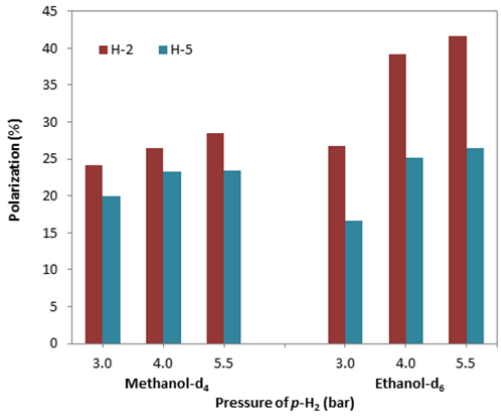

Fig. 5: Effect of *p*-H_2 pressure on the SABRE hyperpolarization of **2b** (4 eq.) with [IrCl(COD)(d_{22}-IMes)] (5 mM) in methanol-d_4 and ethanol-d_6.

Increasing SABRE hyperpolarization by using a co-ligand

Our final consideration in optimizing SABRE catalysis was to overcome the presence of multiple copies of the agent being attached simultaneously to a single iridium center and thus diluting any polarization coming from *p*-H_2. This would require a catalyst redesign, but if a co-ligand is added which cannot itself receive polarization a suitable test scenario can be established. Thus, SABRE hyperpolarization was conducted using a single equivalent of **2b** and three equivalents of methyl-2,4,5,6-d_4-nicotinate, relative to [IrCl(COD)(d_{22}-IMes)] under 5.5 bar *p*-H_2 pressure. This led to 50% polarization being achieved in the H-2 site of **2b**, with an average of 45% across the two sites. This is a truly remarkable result as it is delivered after just 10 seconds of SABRE. Hence we believe that this strategy reflects a compelling route to achieve hyperpolarization which can undoubtedly be improved on even further through higher pressures and a superior catalyst.

Solvent effect on relaxation times

The efficiency of SABRE catalysis has been shown to be highly dependent on the solvent, with low hyperpolarization levels resulting in 100% D_2O solutions despite the development of water soluble catalysts.(32, 33, 36, 37) We suggest that hyperpolarization in an ethanol-d_6 solution followed by sample dilution to obtain a biocompatible bolus for injection reflects a sensible route to obtain the required signal strength for *in vivo* study. The T_1 values of **2b** were measured in ethanol-d_6–D_2O solvent mixtures (see supporting information). Despite the reduction in T_1 values for the H-2 and H-5 signals of **2b** in the mixed solvent systems, in a biocompatible mixture of 10% ethanol-d_6 in D_2O the T_1 value for H-5 remains above 30 seconds. Hence very high levels of hyperpolarization are expected to survive the point of injection. We have measured the T_1 values of H-2 and H-5 in **2b** in water (containing 5% D_2O) at 9.4 T, and they fall to 6.6 and 9.3 s respectively. These values suggest that a detectable signal will be visible *in vivo* for at least 20 s, although if these approached were to be used in drug/urine screening or in analytical NMR more generally there would be no issue with the decay of signal prior to measurement.

Expanding the range of substrates

We have also established the generality of this method by testing a range of additional substrates. To capture a suitable cross section of targets, we have employed materials bearing the nitrogen heterocyclic motifs, pyridazine (**3**), pyrimidine (**4**) and pyrazine (**5**) alongside isonicotinamide (**6**). The best performing isotopologues are presented in Fig. 6 and full data, including effective T_1 relaxation times in the presence of the catalyst can be found in the supporting information. In all cases, the relaxation times and polarization levels are increased. For 3,5-d_2-pyridazine (**3a**), the relaxation time is increased by 550% and the polarization level by 1630% relative to pyridazine (**3**). Similar effects were found for pyrimidine (**4**), where the deuterated isotopologue **4a** yields 4.8% polarization and a signal with a T_1 value of over 2 minutes. Comparison of pyrazine (**5**) to 2,5-d_2-pyrazine (**5a**) shows a relaxation time increase from 32.3 seconds to 86.2 seconds and a polarization level improvement from 3.3% to 11.6%. Finally, 2,5-d_2-isonicotinamide (**6a**) gives a *ca*. 5-fold improvement in T_1 and 80- and 6-fold improvements in polarization levels for H-3 and H-6 respectively over **6**.

These data show, therefore, that the strategy we detail to optimize the SABRE technology is applicable to a broad range of structural motifs and we suggest that most agents that have a need to be studied using either analytical NMR or in a clinical setting will benefit from isotope labelling. Table s5 in the supplementary information details the corresponding T_1 values in a 95% H_2O, 5% D_2O solution, with **2b**, **2c**, **3a**, **4a** and **5a** being the most likely to be detectable *in vivo*.

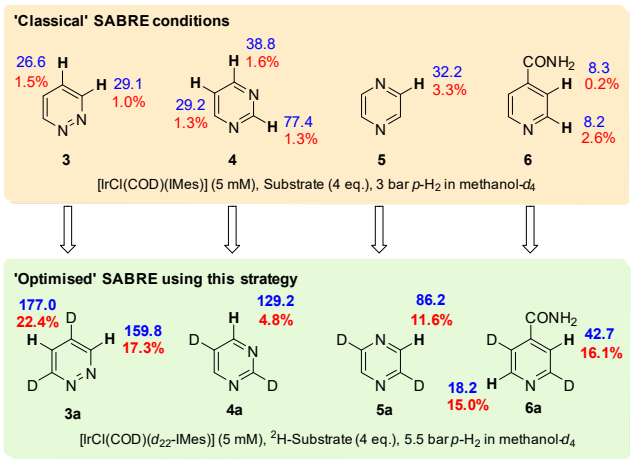

Fig. 6: The change in $T_{1(\text{no cat})}$ (in blue, seconds) and SABRE polarization (in red, percentage) of a range of substrates in methanol-d_4 solution to illustrate the general benefits of ^{2}H labelling. SABRE conditions were: [IrCl(COD)(IMes)] (5

mM), substrate (4 eq.), 3 bar p-H_2. (IMes = 1,3-bis(2,4,6-trimethylphenyl)-imidazol-2-ylidene)

Assessing the impact of these changes for MRI detection

Images of the resultant SABRE derived ^{1}H magnetization of **1** and **2**, and their better performing deuterated analogues, have been collected at 9.4 T in conjunction with a 100 mM substrate concentration in ethanol-d_6. Analogous results under reversible flow, where measurement-repeat is possible, are also detailed in the supporting information and confirm that deuteration not only improves the resultant image intensity relative to their parents but also extends the duration over which visible signals can be detected. The longer T_1 values that these agents exhibit which act to inhibit standard multi-pulse-recovery observations are now of benefit because they should enable detection after *in-vivo* injection and transport to a region of clinical interest. Additionally, this change allows longer echo times to be employed which results in a lower duty cycle and radio frequency deposition rate.

We have also been able to show that when high-contrast is desired, hyperpolarized signals can be observed in the presence of a water phantom whose signal can initially be suppressed to further improve the dynamic range of the image. In the cases of **1f** and **2b**, the hyperpolarized agents are visible 30 seconds after completion of the polarization step with superior image intensity than that of the residual water signal. Furthermore, when **2b** was examined after polarization transfer by [IrCl(COD(d_{22}-IMes)] under 7 bar of p-H_2 the corresponding RARE(38) images of the same samples under normal conditions would take 9 and 40 days of continuous averaging in ethanol-d_6 and methanol-d_4 respectively to reproduce the hyperpolarized results (Fig. 7) that are collected less than 20 seconds after the start of hyperpolarization. Hence we can conclude that the MRI assessment of these agents without hyperpolarization would be impractical. We also compared these data to that obtained for an excised spleen and noted a 30-fold S/N improvement relative to the tissue's H_2O signal.

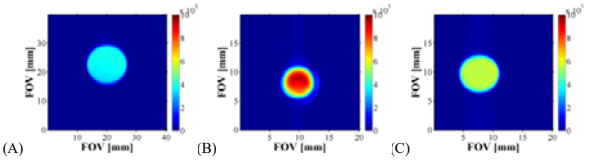

Fig. 7: Hyperpolarized images of methyl nicotinate using [IrCl(COD)(d_{22}-IMes)] under 7 bar p-H_2: (A) Control image of a tube of water; (B) SABRE hyperpolarized image of a sample of **2b** (100 mM in methanol-d_4); (C) analogous SABRE hyperpolarized image of a sample of **2b** (100 mM in ethanol-d_6). Image SNR values are 1586, 4085 and 2955 respectively. Data were acquired under identical conditions and results are plotted on the same scale.

Conclusions

The results presented here suggest that placing a proton next to nitrogen is most desirable for efficient magnetization transfer *via* SABRE while having an isolated proton environment is desirable for a long signal lifetime. In the case of nicotinamide (**1**) and methyl nicotinate (**2**), the deuterated forms that hyperpolarize optimally correspond to **1f** and **2b**. This is because polarization flows from the hydride ligands in the catalyst through to the bound substrates receptor protons optimally when both their spin-spin coupling and relaxation times are maximized. When [IrCl(COD)(IMes)] is used as the catalyst precursor, 10% polarization in **2b** was achieved for H-2. It has also been shown that the catalyst also relaxes the hyperpolarization it creates, an effect which can be reduced when it is ^{2}H-labelled which more than doubles the level of delivered hyperpolarization to 22% when [IrCl(COD)(d_{22}-IMes)] is employed. Increasing the p-H_2 pressure from 3 to 5.5 bar further increases this to 41%, while 50% H-2 polarization of **2b** can be achieved with the co-ligand methyl-2,4,5,6-$\boldsymbol{d_4}$-nicotinate.

Given that the hyperpolarization process associated with SABRE is continuous,(23, 39) we predict it would be possible to complete any offline analyses needed to establish viability for future *in vivo* use, such as a pH assessment, prior to injection and the start of relaxation. Furthermore, by using the synthetic strategy we have described a hyperpolarized agent with ca. 50 % magnetic state purity (longitudinal magnetization), which is 100,000 times bigger than the 0.0005% level of a 1.5 T hospital scanner, has been produced on a single spin in just a few seconds. The resulting hyperpolarized and slowly relaxing magnetization has also been harnessed productively in a series of MRI experiments that establish these performance improvements are maintained and that our optimized agents can deliver signals which are over one order of magnitude stronger than that of biological tissue. In order to harness these results, an automated delivery system needs to be assembled to enable the injection of these agents which integrates the final steps of sample dilution and catalyst deactivation and removal to ensure biocompatibility. We also expect that these levels of enhancement can be increased still further under conditions where p-H_2 is no longer limiting. We are currently using this approach to optimally polarize ^{13}C and ^{15}N nuclei to extend the magnetization lifetimes and polarization levels of other nuclei.

Consequently, if we were to assume that 20 seconds are required from the point of injection to starting an MRI measurement, for a nominal initial polarization level of 50% we would be left with *ca*. 7% if the T_1 value was maintained at 10 seconds *in vivo*. For comparison purposes, pyruvate, delivered with a typical 30% ^{13}C polarization level and an *in vivo* T_1 of 30 seconds retains 11% polarization at this point.(40) The levels of polarization achieved here by SABRE is therefore fully commensurate with that needed for future *in vivo* success, particularly given the higher sensitivity of ^{1}H nuclei, rather than ^{13}C nuclei.

At a molecular level, we have developed and demonstrated a strategy to optimize the detection levels of a SABRE-hyperpolarized biomarker. This has required the production of a range of ^{2}H-labelled substrates, and the selection of their optimal form based on their relaxation time and SABRE hyperpolarization level. A combination of these procedures, with subsequent sample dilution, reflects a viable route to produce a biocompatible bolus for *in vivo* measurement. We are also using this approach to improve on low concentration NMR detectability for analytical purposes in a similar way. Furthermore, by illustrating the success of this approach for a variety of agents we believe that we articulate a general strategy to maximize both polarization amplitude and lifetime which will be useful to others.

Materials and Methods

Synthesis and Reactivity Studies All reactions utilizing air- and moisture-sensitive reagents were performed in dried glassware under an atmosphere of dry nitrogen. Dry solvents (THF, Toluene and DCM) were obtained from a Braun MB-SPS-800. For thin-layer

chromatography (TLC) analysis, Merck pre-coated plates (silica gel 60 F254, Art 5715, 0.25 mm) were used. Column chromatography was performed on Fluka Silica gel (60 Å, 220-440 mesh). Deuterated solvents (methanol-d_4, ethanol-d_6 and D_2O) were obtained from Sigma-Aldrich and used as supplied. Detailed synthetic procedures and characterization data can be found in the supplementary material.

Hyperpolarization studies ^{1}H NMR spectra in addition to the relaxation data were measured on a Bruker 400 MHz spectrometer. SABRE hyperpolarization transfer experiments involved *p*-H_2 that was produced by cooling H_2 gas over Fe_2O_3 at 30 K. Samples contained 5 mM concentrations of the catalyst and 5 up to 20 equivalents of substrate relative to iridium in the specified solvent in a 5 NMR tube fitted with a J. Young's Tap. The resulting solutions were degassed prior to the introduction of *p*-H_2 at a pressure of 3 bar unless otherwise stated. Samples were shaken for 7 seconds in a specified fringe field of a 9.4 T Bruker Avance (III) NMR spectrometer for hyperpolarization transfer prior to being rapidly transported into the main magnetic field of the instrument for subsequent probing by NMR or MRI methods. The associated polarization transfer experiment data can be found in the supplementary material.

Statistical Analysis Errors have been calculated using the standard deviation formula, taking into account the limited number of population samples. Gaussian error propagation has been assumed (see supporting information).

Acknowledgements

This work was supported by The Wellcome Trust (Grants 092506 and 098335), Bruker Biospin UK and the University of York. We also thank Professor V. H. Perry for useful discussions. Ryan Mewis is now based at Manchester Metropolitan University.

Author Contributions

P.J.R., M.J.B., A.M.O and S.B.D. conceived and designed the experiments. P.J.R, M.J.B and P.N synthesised and characterised non-commercial substrates and catalysts. P.J.R, M.J.B, P.N, M.F and R.E.M. performed and analysed NMR measurements. A.M.O and L.A.R.H performed and analysed the MRI experiments. P.J.R, M.J.B, A.M.O and S.B.D wrote the manuscript with interpretation and input from all authors. S.B.D. and G.G.R.G. provided supervision.

1. Kurhanewicz J*, et al.* (2011) Analysis of Cancer Metabolism by Imaging Hyperpolarized Nuclei: Prospects for Translation to Clinical Research. *Neoplasia* 13(2):81-97.
2. Gutte H*, et al.* (2015) The use of dynamic nuclear polarization (13)C-pyruvate MRS in cancer. *American journal of nuclear medicine and molecular imaging* 5(5):548-560.
3. Comment A & Merritt ME (2014) Hyperpolarized Magnetic Resonance as a Sensitive Detector of Metabolic Function. *Biochemistry* 53(47):7333-7357.
4. Ardenkjær-Larsen JH*, et al.* (2003) Increase in signal-to-noise ratio of > 10,000 times in liquid-state NMR. *Proceedings of the National Academy of Sciences* 100(18):10158-10163.
5. Nikolaou P*, et al.* (2013) Near-unity nuclear polarization with an open-source Xe-129 hyperpolarizer for NMR and MRI. *Proceedings of the National Academy of Sciences of the United States of America* 110(35):14150-14155.
6. Lee Y (2016) Dissolution dynamic nuclear polarization-enhanced magnetic resonance spectroscopy and imaging: Chemical and biochemical reactions in nonequilibrium conditions. *Appl. Spectrosc. Rev.* 51(3):190-206.
7. Nikolaou P*, et al.* (2014) XeNA: An automated 'open-source' Xe-129 hyperpolarizer for clinical use. *Magnetic Resonance Imaging* 32(5):541-550.
8. Duckett SB & Mewis RE (2012) Application of Parahydrogen Induced Polarization Techniques in NMR Spectroscopy and Imaging. *Accounts of Chemical Research* 45(8):1247-1257.
9. Green RA*, et al.* (2012) The theory and practice of hyperpolarization in magnetic resonance using parahydrogen. *Progress in Nuclear Magnetic Resonance Spectroscopy* 67:1-48.
10. Bowers CR & Weitekamp DP (1987) Parahydrogen and synthesis allow dramatically enhanced nuclear alignment. *Journal of the American Chemical Society* 109(18):5541-5542.
11. Anwar MS*, et al.* (2004) Preparing high purity initial states for nuclear magnetic resonance quantum computing. *Physical Review Letters* 93(4).
12. Beckonert O*, et al.* (2007) Metabolic profiling, metabolomic and metabonomic procedures for NMR spectroscopy of urine, plasma, serum and tissue extracts. *Nat. Protoc.* 2(11):2692-2703.
13. Reile I*, et al.* (2016) NMR detection in biofluid extracts at sub-mu M concentrations via para-H-2 induced hyperpolarization. *Analyst* 141(13):4001-4005.
14. Eshuis N*, et al.* (2014) Toward Nanomolar Detection by NMR Through SABRE Hyperpolarization. *Journal of the American Chemical Society* 136(7):2695-2698.
15. Adams RW*, et al.* (2009) Reversible Interactions with para-Hydrogen Enhance NMR Sensitivity by Polarization Transfer. *Science* 323(5922):1708-1711.
16. Frydman L (2009) Chemistry awakens a silent giant. *Nat. Chem.* 1(3):176-178.
17. Shchepin RV*, et al.* (2016) N-15 Hyperpolarization of Imidazole-N-15(2) for Magnetic Resonance pH Sensing via SABRE-SHEATH. *Acs Sensors* 1(6):640-644.
18. Logan AWJ, Theis T, Colell JFP, Warren WS, & Malcolmson SJ (2016) Hyperpolarization of Nitrogen-15 Schiff Bases by Reversible Exchange Catalysis with para-Hydrogen. *Chemistry-a European Journal* 22(31):10777-10781.
19. Truong ML*, et al.* (2015) N-15 Hyperpolarization by Reversible Exchange Using SABRE-SHEATH. *Journal of Physical Chemistry C* 119(16):8786-8797.
20. Zeng HF*, et al.* (2013) Optimization of SABRE for polarization of the tuberculosis drugs pyrazinamide and isoniazid. *Journal of Magnetic Resonance* 237:73-78.
21. Ducker EB, Kuhn LT, Munnemann K, & Griesinger C (2012) Similarity of SABRE field dependence in chemically different substrates. *Journal of Magnetic Resonance* 214:159-165.
22. Hovener J-B*, et al.* (2013) A hyperpolarized equilibrium for magnetic resonance. *Nature Communications* 4:2946-2946.
23. Rovedo P*, et al.* (2016) Molecular MRI in the Earth's Magnetic Field Using Continuous Hyperpolarization of a Biomolecule in Water. *The Journal of Physical Chemistry B* 120(25):5670-5677.
24. MacKay D, Hathcock J, & Guarneri E (2012) Niacin: chemical forms, bioavailability, and health effects. *Nutrition Reviews* 70(6):357-366.
25. Allouche-Arnon H, Lerche MH, Karlsson M, Lenkinski RE, & Katz-Brull R (2011) Deuteration of a molecular probe for DNP hyperpolarization - a new approach and validation for choline chloride. *Contrast Media & Molecular Imaging* 6(6):499-506.
26. Mewis RE, Fekete M, Green GGR, Whitwood AC, & Duckett SB (2015) Deactivation of signal amplification by reversible exchange catalysis, progress towards in vivo application. *Chemical Communications* 51(48):9857-9859.

27. Mewis RE*, et al.* (2014) Probing signal amplification by reversible exchange using an NMR flow system. *Magnetic Resonance in Chemistry* 52(7):358-369.
28. Cowley MJ*, et al.* (2011) Iridium N-Heterocyclic Carbene Complexes as Efficient Catalysts for Magnetization Transfer from para-Hydrogen. *Journal of the American Chemical Society* 133(16):6134-6137.
29. Jiang W*, et al.* (2015) Hyperpolarized 15N-pyridine Derivatives as pH-Sensitive MRI Agents. *Scientific Reports* 5:9104.
30. Theis T*, et al.* (2015) Microtesla SABRE Enables 10% Nitrogen-15 Nuclear Spin Polarization. *Journal of the American Chemical Society* 137(4):1404-1407.
31. Shchepin RV, Barskiy DA, Mikhaylov DM, & Chekmenev EY (2016) Efficient Synthesis of Nicotinamide-1-15N for Ultrafast NMR Hyperpolarization Using Parahydrogen. *Bioconjugate Chemistry* 27(4):878-882.
32. Fekete M*, et al.* (2015) Utilisation of water soluble iridium catalysts for signal amplification by reversible exchange. *Dalton Transactions* 44(17):7870-7880.
33. Spannring P*, et al.* (2016) A New Ir-NHC Catalyst for Signal Amplification by Reversible Exchange in D2O. *Chemistry – A European Journal* 22(27):9277-9282.
34. Eshuis N*, et al.* (2016) Determination of long-range scalar (1)H-(1)H coupling constants responsible for polarization transfer in SABRE. *Journal of magnetic resonance (San Diego, Calif. : 1997)* 265:59-66.
35. Lloyd LS*, et al.* (2014) Hyperpolarisation through reversible interactions with parahydrogen. *Catalysis Science & Technology* 4(10):3544-3554.
36. Shi F*, et al.* (2016) Aqueous NMR Signal Enhancement by Reversible Exchange in a Single Step Using Water-Soluble Catalysts. *The Journal of Physical Chemistry C* 120(22):12149-12156.
37. Hövener J-B*, et al.* (2014) Toward Biocompatible Nuclear Hyperpolarization Using Signal Amplification by Reversible Exchange: Quantitative in Situ Spectroscopy and High-Field Imaging. *Analytical Chemistry* 86(3):1767-1774.
38. Hennig J, Nauerth A, & Friedburg H (1986) Rare Imaging - A Fast Imaging Method for Clinical MR. *Magnetic Resonance in Medicine* 3(6):823-833.
39. Hoevener J-B*, et al.* (2013) A hyperpolarized equilibrium for magnetic resonance. *Nature Communications* 4.
40. Chen WC, Teo XQ, Lee MY, Radda GK, & Lee P (2015) Robust hyperpolarized C-13 metabolic imaging with selective non-excitation of pyruvate (SNEP). *Nmr in Biomedicine* 28(8):1021-1030.

Table 1. Hyperpolarization and T_1 data for nicotinamide (**1**) and the seven ^{2}H-labelled analogues **1a-1g**. SABRE catalysis performed with 5 mM [IrCl(COD)(IMes)] (IMes = 1,3-bis(2,4,6-trimethylphenyl)-imidazol-2-ylidene), 4 equivalents of agent, under 3 bar p-H_2 in methanol-d_4 or ethanol-d_6 at 298K. T_1 measurements without catalyst were on a degassed sample containing 20 mM of agent. Errors are <5% unless otherwise specified.

Agent	Methanol-d_4			Ethanol-d_6			D_2O
	Site $T_{1(\text{no cat.})}$ / s	Site $T_{1(\text{eff., with cat.})}$ /s	Polarization Level (%)	Site $T_{1(\text{no cat.})}$ / s	Site $T_{1(\text{eff., with cat.})}$ /s	Polarization Level (%)	T_1 / s
1 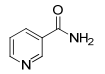	H-2: 16.3 H-4: 11.3 H-5: 6.9 H-6: 9.8	H-2: 6.2 H-4: 6.3 H-5: 3.7 H-6: 3.8	H-2: 2.1 H-4: 2.0 H-5: 0.6 H-6: 1.9	H-2: 24.3 H-4: 6.7 H-5: 3.9 H-6: 7.8	H-2: 4.2 H-4: 3.9 H-5: 2.4 H-6: 2.7	H-2: 1.1 H-4: 0.8 H-5: 0.1 H-6: 1.0	H-2: 10.7 H-4: 8.9 H-5: 6.5 H-6: 7.5
1a 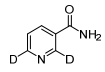	H-4: 11.2 H-5: 11.0	H-4: 5.8 H-5: 5.8	H-4: 0.2 H-5: 0.05	H-4: 6.1 H-5: 6.2	H-4: 3.8 H-5: 3.8	H-4: 0.1 H-5: 0.05	H-4: 11.2 H-5: 11.3
1b 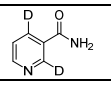	H-5: 14.5 H-6: 10.9	H-5: 5.8 H-6: 3.5	H-5: 2.4 H-6: 2.4	H-5: 7.3 H-6: 6.8	H-5: 5.1 H-6: 0.5	H-5: 0.3 H-6: 0.2	H-5: 12.2 H-6: 9.5
1c 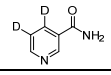	H-2: 14.8 H-6: 17.0	H-2: 3.7 H-6: 0.4	H-2: 1.7 H-6: 1.3	H-2: 13.5 H-6: 16.0	H-2: 3.2 H-6: 3.4	H-2: 0.9 H-6: 0.6	H-2: 39.4 H-6: 37.9
1d 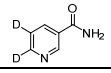	H-2: 8.1 H-4: 55.8	H-2: 6.7 H-4: 25.1	H-2: 2.1 H-4: 2.4	H-2: 8.1 H-4: 30.1	H-2: 3.3 H-4: 9.3	H-2: 0.6 H-4: 0.7	H-2: 13.0 H-4: 63.5
1e 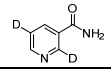	H-4: 63.5 H-6: 70.4	H-4: 18.9 H-6: 2.0	H-4: 2.7 H-6: 3.2	H-4: 28.0 H-6: 28.4	H-4: 14.6 H-6: 1.9	H-4: 1.9 H-6: 1.9	H-4: 51.8 H-6: 35.2
1f 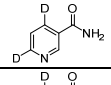	H-2: 26.8 H-5: 47.9	H-2: 7.9 H-5: 20.4	H-2: 4.1 H-5: 4.1	H-2: 22.2 H-5: 37.5	H-2: 8.2 H-5: 17.5	H-2: 2.0 H-5: 2.1	H-2: 37.1 H-5: 54.0
1g 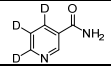	H-2: 45.7	H-2: 5.9	H-2: 2.1	H-2: 25.7	H-2: 3.8	H-2: 0.4	H-2: 28.5

Table 2. Hyperpolarization and T_1 data for methyl-nicotinate (**2**) and the four ^{2}H-labelled analogues **2a-2d**. SABRE catalysis performed with 5 mM [IrCl(COD)(IMes)] (IMes = 1,3-bis(2,4,6-trimethylphenyl)-imidazol-2-ylidene), 4 equivalents of agent, under 3 bar p-H_2 in methanol-d_4 or ethanol-d_6 at 298K. T_1 measurements without catalyst were on a degassed sample containing 20 mM of agent. Errors are <5% unless otherwise specified.

Agent	Methanol-d_4			Ethanol-d_6			D_2O
	Site $T_{1(\text{no cat.})}$ /s	Site $T_{1\ (\text{eff., with cat.})}$ /s	Polarization Level /%	Site $T_{1(\text{no cat.})}$ / s	Site $T_{1(\text{eff. with cat.})}$ /s	Polarization Level /%	T_1 / s
2 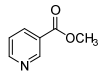	H-2: H- 59.8 4: 22.0 H- 12.6 5: 21.4 H- 6:	H- 2: H- 4.9 4: 6.5 H- 3.6 5: 3.1 H- 6:	H-2: 3.7 H-4: 3.1 H-5: 1.3 H-6: 3.0	H- 2: H- 48.9 4: 14.4 H- 8.1 5: 14.1 H- 6:	H- 2: H- 8.0 4: 5.2 H- 4.9 5: 8.7 H- 6:	H-2: 2.6 H-4: 1.7 H-5: 0.7 H-6: 1.9	H- 2: H- 13.8 4: 8.3 H- 6.2 5: 8.7 H- 6:
2a 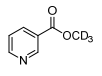	H- 2: H- 67.2 4: 22.3 H- 12.4 5: 21.0 H- 6:	H- 2: H- 5.3 4: 3.1 H- 7.0 5: 3.1 H- 6:	H-2: 5.8 H-4: 5.3 H-5: 1.4 H-6: 4.1	H- 2: H- 31.0 4: 13.9 H- 7.9 5: 12.3 H- 6:	H- 2: H- 14.9 4: 8.3 H- 4.9 5: 5.1 H- 6:	H-2: 1.5 H-4: 1.1 H-5: 0.5 H-6: 1.1	H- 2: H- 37.1 4: 8.9 H- 6.8 5: 12.2 H- 6:
2b 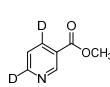	H- 2: 65.7 H- 97.6 5:	H- 2: 5.8 H- 20.9 5:	H-2: 10.1 H-5: 9.5	H- 2: 46.2 H- 62.7 5:	H- 2: 6.8 H- 18.8 5:	H-2: 9.3 H-5: 8.2	H- 2: 30.9 H- 47.4 5:

2c	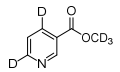	H-2: 116.0 H-5: 107	H-2: 6.6 H-5: 23.8	H-2: 9.5 H-5: 8.3	H-2: 49.8 H-5: 66.3	H-2: 5.5 H-5: 15.6	H-2: 7.5 H-5: 7.0	H-2: 50.1 H-5: 50.3
2d	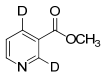	H-5: 26.0 H-6: 20.6	H-5: 5.5 H-6: 4.7	H-5: 3.7 H-6: 4.0	H-5: 16.7 H-6: 14.6	H-5: 5.5 H-6: 3.6	H-5: 2.7 H-6: 2.9	H-5: 15.7 H-6: 14.2
2e	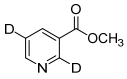	H-4: 94.3 H-6: 64.4	H-4: 28.2 H-6: 6.8	H-4: 11.0 H-6: 9.5	H-4: 61.2 H-6: 47.9	H-4: 24.6 H-6: 9.2	H-4: 6.2 H-6: 6.1	H-4: 44.2 H-6: 48.8

Table 3: Effective T_1 values for protons H-2 and H-5 in methyl-4,6-d_2-nicotinate **2b** (20mM loading), and the corresponding equatorial and axial ligands of the SABRE catalyst with [IrCl(COD)(NHC)] (where NHC = IMes, d_2-, d_{22}- or d_{24}-IMes, at 5 mM loading) and H_2 or D_2 (3 bar) in methanol-d_4 solution at 263 K.

NHC	**IMes** $T_{1(\text{eff., with cat.})}$/s				**d_2-IMes** $T_{1(\text{eff., with cat.})}$/s				**d_{22}-IMes** $T_{1(\text{eff., with cat.})}$/s				**d_{24}-IMes** $T_{1(\text{eff., with cat.})}$/s			
Gas	**H_2**		**D_2**		**H_2**		**D_2**		**H_2**		**D_2**		**H_2**		**D_2**	
2b	H-2:	10.6	H-2:	10.9	H-2:	13.1	H-2:	13.8	H-2:	13.5	H-2:	20.1	H-2:	12.1	H-2:	14.1
	H-5:	18.4	H-5:	18.3	H-5:	20.3	H-5:	25.3	H-5:	23.2	H-5:	23.7	H-5:	21.0	H-5:	30.9
Equatorially Bound **2b**	H-2:	1.4	H-2:	1.9	H-2:	2.0	H-2:	1.5	H-2:	2.0	H-2:	2.6	H-2:	3.2	H-2:	2.3
	H-5:	6.7	H-5:	5.6	H-5:	6.7	H-5:	6.5	H-5:	9.0	H-5:	7.3	H-5:	12.0	H-5:	10.5
Axially Bound **2b**	H-2:	1.9	H-2:	4.1	H-2:	1.7	H-2:	3.6	H-2:	2.5	H-2:	4.8	H-2:	1.7	H-2:	4.0
	H-5:	2.3	H-5:	2.4	H-5:	4.0	H-5:	2.7	H-5:	8.0	H-5:	3.8	H-5:	12.3	H-5:	10.1

Table 4: Effect of ^{2}H-labelling the catalyst on the effective T_1 values and polarization levels of H-2 and H-5 in **2b** under SABRE catalysis by [IrCl(COD)(NHC)] (where NHC = d_2-, d_{22}- or d_{24}-IMes) with 3 bar p-H_2 at 298 K.

NHC	**Methanol-d_4**				**Ethanol-d_6**			
	$T_{1(\text{eff., with cat.})}$/s		**Polarization /%**		**$T_{1(\text{eff., with cat.})}$/s**		**Polarization /%**	
d_2-IMes	H-2:	5.8	H-2:	10.1	H-2:	5.5	H-2:	9.3
	H-5:	20.9	**H-5:**	9.5	**H-5:**	15.6	**H-5:**	8.2
d_{22}-IMes	H-2:	7.7	H-2:	24.1	H-2:	7.7	H-2:	26.8
	H-5:	26.6	**H-5:**	19.9	**H-5:**	17.2	**H-5:**	16.6
d_{24}-IMes	H-2:	9.5	H-2:	18.6	H-2:	7.5	H-2:	13.3
	H-5:	33.5	**H-5:**	16.5	**H-5:**	19.3	**H-5:**	8.2

Delivering Strong ^{1}H Nuclei Hyperpolarization Levels and Long Magnetic Lifetimes through Signal Amplification by Reversible Exchange

Peter J. Rayner, Michael J. Burns, Alexandra M. Olaru, Philip Norcott, Marianna Fekete, Gary G. R. Green, Louise A. R. Highton, Ryan. E. Mewis and Simon. B. Duckett*

Centre for Hyperpolarisation in Magnetic Resonance, Department of Chemistry, University of York, Heslington, YO10 5NY

1. Synthesis and characterisation

- **1.1 General**
- **1.2 General Procedures**
- **1.3 Synthetic procedures and characterisation data**

2. NMR experiments

- **2.1 Polarization transfer methods**
- **2.2 ^{1}H Enhancement factors calculation and statistical analysis**
- **2.3 Representative NMR spectra of the SABRE effect in deuterated agents**
- **2.4 Polarisation transfer with deuterated IMes catalysts**
- **2.5 Effect of *p*H_2 pressure on polarisation with [IrCl(COD)(d_{22}-IMes)]**
- **2.6 Use of methyl-2,4,5,6-d_4-nicotinate as a co-substrate**
- **2.7 Kinetic behaviour of 2b with [IrCl(COD)(NHC)] under H_2**
- **2.8 T_1 relaxation data for 2b in ethanol-d_6:D_2O solvent mixtures**
- **2.9 T_1 relaxation data in H_2O solution containing 5% D_2O**

3. SABRE MRI Collection

- **3.2 MRI Instrumentation and Procedures**
  - **3.2.1 MRI instrumentation**
  - **3.2.2 MRI acquisition methods**
  - **3.2.3 MRI data processing and statistical analysis**
- **3.3 Results**
  - **3.3.1 Image intensity optimisation through selective deuteration**
  - **3.3.2 Effects of relaxation on image quality**
  - **3.3.3 Image contrast optimisation by water and solvent suppression**
  - **3.3.4 Effects of *p*H_2 pressure on image quality**

1. Synthesis and characterisation

1.1 General

Water is distilled water. Brine refers to a saturated aqueous solution of NaCl. THF was freshly distilled from sodium and benzophenone ketyl or dried using a Grubbs solvent purification system. Petrol refers to the fraction of petroleum ether boiling in the range 40-60 °C. All reactions were carried out under O_2-free Ar or N_2 using oven-dried and/or flame-dried glassware.

Flash column chromatography was carried out using Fluka Chemie GmbH silica (220-440 mesh). Reverse-phase flash column chromatography was carried out using a Biotage Isolera with a SNAP-C_{18}-12g cartridge eluting with H_2O-MeCN containing 0.1% NH_4OH. Thin layer chromatography was carried out using Merck F_{254} aluminium-backed silica plates. ^1H (400 MHz) and ^{13}C (100.6 MHz) NMR spectra were recorded on a Bruker-400 instrument with an internal deuterium lock. Chemical shifts are quoted as parts per million and referenced to $CHCl_3$ (δ_H 7.27), $(CH_3)_2SO$ (δ_H 2.54), $CDCl_3$ (δ_C 77.0) or $(CD_3)_2SO$ (δ_C 40.45). ^{13}C NMR spectra were recorded with broadband proton decoupling. ^{13}C NMR spectra were assigned using DEPT experiments where necessary. Coupling constants (*J*) are quoted in Hertz. Electrospray high and low resolution mass spectra were recorded on a Bruker Daltonics microOTOF spectrometer.

All compounds were purchased from Sigma-Aldrich, Fluorochem or Alfa-Aesar and used as supplied unless otherwise stated. The following compounds were synthesised according to literature procedures; methyl-2,4-dichloronicotinate,(1) ethyl-4,5,6-trichloronicotinate,(2) and [IrCl(COD)(IMes)].(3)

1.2 General Procedures

General Procedure A – Deuteration of heteroaryl chlorides

5% Pd/C (10 wt%) was added to a stirred suspension of heteroaryl chloride (1.0 eq.) and K_2CO_3 (2.5 - 3.5 eq.) in MeOD (10 mL) or EtOD (10 mL) in a 30 mL Parr Reactor. The Parr reactor was sealed, purged with $N_{2(g)}$ and pressurised with $D_{2(g)}$ (5 bar). The reaction was then stirred at rt for 3 h. Then, the pressure was released and the suspension was filtered through Celite® and washed with CH_2Cl_2. The filtrate was concentrated under reduced pressure to give the crude product.

General Procedure B – Synthesis of nicotinamide by amide formation

The nicotinate (1.0 eq) was dissolved in ammonia (10 mL of a 7 N solution in MeOH) and the resulting solution stirred at rt for 2 days. The solution was concentrated under reduced pressure to give the crude product.

1.3 Synthetic procedures and characterisation data

Methyl-2,6-d_2-nicotinate S1

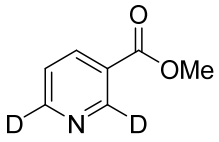

S1

Using General Procedure A, methyl-2,6-dichloronicotinate (100 mg, 0.485 mmol, 1.0 eq.), 5% Pd/C (10 mg, 10 wt%), K_2CO_3 (167 mg, 1.21 mmol, 2.5 eq.) and $D_{2(g)}$ (5 bar) in THF (10 mL) gave the crude product. Purification by flash column chromatography with 1:1 petrol-EtOAc as eluent gave methyl-2,6-d_2-nicotinate **S1** (43 mg, 63%) as a pale yellow solid, R_F (1:1 petrol-EtOAc) 0.3; **^{1}H NMR** (400 MHz, $CDCl_3$) δ (ppm) 8.30 (d, J = 8.1 Hz, 1H), 7.40 (d, J = 8.1 Hz, 1H), 3.96 (s, 3H); **^{13}C NMR** (101 MHz, $CDCl_3$) δ (ppm) 165.8 (s), 153.1 (t, J = 28.1 Hz), 150.5 (t, J = 28.1 Hz), 137.1 (s), 125.9 (s), 123.2 (s), 52.4 (s); **MS** (ESI) m/z 140 [(M + H)$^+$, 100]; **HRMS** (ESI) m/z [M + H]$^+$ calculated for $C_7H_6D_2NO_2$ 140.0675, found 140.0674 (−1.8 ppm error).

2,6-d_2-Nicotinamide 1a

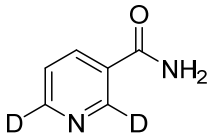

1a

Using General Procedure B, methyl-2,6-d_2-nicotinate **S1** (45 mg, 0.324 mmol) in ammonia (6 mL of a 7 N solution in MeOH) gave the crude product. Purification by reverse phase flash column chromatography (0-30% MeCN) gave 2,6-d_2-nicotinamide **1a** (34 mg, 85%) as a white solid, **^{1}H NMR** (400 MHz, d_6-DMSO) δ (ppm) 8.22 (d, J = 8.0 Hz, 1H), 8.21 (br s, 1H), 7.62 (br s, 1H) 7.50 (d, J = 8.0 Hz, 1H); **^{13}C NMR** (101 MHz, d_6-DMSO) δ (ppm) 166.9 (s), 152.0 (t, J = 26.5 Hz), 148.8 (t, J = 27.0 Hz), 135.7 (s), 130.0 (s), 123.8 (s); **MS** (ESI) m/z 147 [(M + Na)$^+$, 72] 125 [(M + H)$^+$, 100]; **HRMS** (ESI) m/z [M + H]$^+$ calculated for $C_6H_5D_2N_2O$ 125.0678, found 125.0679 (−0.7 ppm error).

Ethyl-2,4-d_2-nicotinate S2

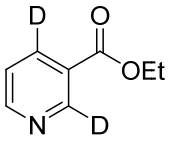

S2

Using General Procedure A, methyl-2,4-dichloronicotinate(1) (135 mg, 0.65 mmol, 1.0 eq.), 5% Pd/C (14 mg, 10 wt%), K_2CO_3 (250 mg, 2.75 mmol, 2.5 eq.) and $D_{2(g)}$ (5 bar) in EtOD (10 mL) gave the crude product. Purification by flash column chromatography with 1:1 petrol-EtOAc as eluent gave ethyl-2,4-d_2-nicotinate **S2** (62 mg, 62%) as a pale yellow oil, R_F (1:1 petrol-EtOAc) 0.3; **^{1}H NMR** (400 MHz, $CDCl_3$) δ (ppm) 8.77-8.75 (m, 1H), 7.38-7.37 (m, 1H),

4.41 (qd, *J* = 7.2, 3.3 Hz, 2H), 1.42-1.38 (m, 3H); **^{13}C NMR** (101 MHz, $CDCl_3$) δ (ppm) 165.2 (s), 153.3 (s), 150.5 (t, *J* = 28.1 Hz), 136.7 (t, *J* = 25.1 Hz), 126.1 (s), 123.1 (s), 61.4 (s), 14.2 (s); **MS** (ESI) *m/z* 154 [$(M + H)^+$, 100], 126 [32]; **HRMS** (ESI) *m/z* $[M + H]^+$ calculated for $C_8H_8D_2NO_2$ 154.0832, found 154.0831 (+1.4 ppm error).

2,4-d_2-Nicotinamide 1b

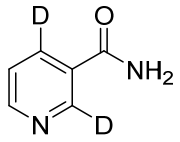

1b

Using General Procedure B, ethyl 2,4-d_2-nicotinate **S2** (62 mg, 0.406 mmol) in ammonia (5 mL of a 7 N solution in MeOH) gave the crude product. Purification by reverse phase flash column chromatography (0-30% MeCN) gave 2,4-d_2-nicotinamide **1b** (50 mg, 100%) as a white solid, **^{1}H NMR** (400 MHz, d_6-DMSO) δ (ppm) 8.70 (d, *J* = 4.6 Hz, 1H), 8.18 (br s, 1H), 7.62 (br s, 1H), 7.50 (d, *J* = 4.6 Hz, 1H); **^{13}C NMR** (101 MHz, d_6-DMSO) δ (ppm) 166.9 (s), 152.4 (s), 148.8 (t, *J* = 27.1 Hz), 135.3 (t, *J* = 26.4 Hz), 129.9 (s), 123.8 (s); **MS** (ESI) *m/z* 147 [$(M + Na)^+$, 45], 125 [$(M + H)^+$, 100]; **HRMS** (ESI) *m/z* $[M + H]^+$ calculated for $C_6H_5D_2N_2O$ 125.0678, found 125.0681 (−1.8 ppm error).

3-Bromo-2,4,5,6-d_4-pyridine *N*-oxide S3

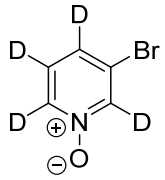

S3

A solution of 3-bromopyridine *N*-oxide (1.07 g, 6.15 mmol), NaOH (100 mg, 2.5 mmol, 0.4 eq.) and D_2O (10 mL) was heated to 180 °C in a microwave for 1 h. The reaction was concentrated under reduced pressure and refreshed with D_2O (10 mL), then heated to 180 °C for a further hour in a microwave. The solvent was removed under reduced pressure and the process repeated an additional time. The reaction was subsequently concentrated under reduced pressure and dissolved in CH_2Cl_2 (50 mL), dried over $MgSO_{4(s)}$, filtered and concentrated under reduced pressure to afford 3-bromo-2,4,5,6-d_4-pyridine *N*-oxide **S3** (1.05 g, 96%) as a pale yellow oil which was used without further purification, **^{13}C NMR** (126 MHz, $CDCl_3$) δ (ppm) 140.7 (t, *J* = 29.3 Hz), 137.8 (t, *J* = 29.0 Hz), 128.4 (t, *J* = 26.6 Hz), 125.6 (t, *J* = 25.7 Hz), 120.4 (s); **MS** (ESI) *m/z* 202 [(^{81}Br-M + Na)$^+$, 70], 200 [(^{79}Br-M + Na)$^+$, 72], 180 [(^{81}Br-M + H)$^+$, 96], 178 [(^{79}Br-M + H)$^+$, 100]; **HRMS** (ESI) *m/z* $[M + H]^+$ calculated for $C_5H^{79}BrD_4NO$ 177.9800, found 177.9805 (−1.4 ppm error).

3-Bromo-4,5-d_2-pyridine *N*-oxide S4

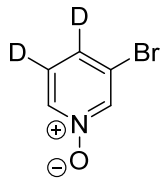

S4

A solution of 3-bromo-2,4,5,6-d_4-pyridine *N*-oxide **S3** (400 mg, 2.25 mmol), K_2CO_3 (200 mg, 1.45 mmol, 0.65 eq.) and H_2O (20 mL) was heated to 100 °C for 16 h. The reaction was concentrated under reduced pressure and dissolved in CH_2Cl_2 (50 mL), dried over $MgSO_{4(s)}$, filtered and concentrated under reduced pressure to afford 3-bromo-4,5-d_2-pyridine *N*-oxide **S4** (334 mg, 84%) as a pale yellow oil used without further purification, **^{1}H NMR** (400 MHz, $CDCl_3$) δ (ppm) 8.35 (s, 1H), 8.14 (s, 1H), 7.40 (s, 0.12 H), 7.16 (d, J = 6.0 Hz, 0.06 H); **^{13}C NMR** (101 MHz, $CDCl_3$) δ (ppm) 140.9 (s), 138.1 (s), 128.4 (t, J = 26.8 Hz), 125.8 (t, J = 25.7 Hz), 120.5 (s); **MS** (ESI) *m/z* 200 [(^{81}Br-M + Na)$^+$, 98], 198 [(^{79}Br-M + Na)$^+$, 100], 178 [(^{81}Br-M + H)$^+$, 71], 176 [(^{79}Br-M + H)$^+$, 70]; **HRMS** (ESI) *m/z* [M + H]$^+$ calculated for $C_5H_3{}^{79}BrD_2NO$ 175.9675, found 175.9670 (+3.9 ppm error).

Methyl 4,5-d_2-nicotinate *N*-oxide S5

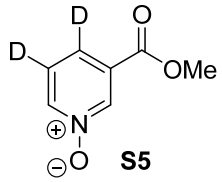

S5

A solution of 3-bromo-4,5-d_2-pyridine *N*-oxide **S4** (180 mg, 1.02 mmol), Et_3N (1 mL, 13.6 mmol, 13.3 eq.), $PdCl_2$(dppf) (20 mg, 0.025 mmol, 2.5 mol%) and MeOH (10 mL) was heated to 75 °C under $CO_{(g)}$ (4 Bar) for 4 h. The reaction was allowed to cool and concentrated under reduced pressure to afford the crude product. Purification by flash column chromatography (0-10% MeOH in CH_2Cl_2) gave methyl-4,5-d_2-nicotinate *N*-oxide **S5** (124 mg, 78%) as a pale yellow waxy solid, R_F (95:5 CH_2Cl_2-MeOH) 0.3; **^{1}H NMR** (400 MHz, $CDCl_3$) δ (ppm) 8.53 (s, 1H), 8.46 (s, 1H), 7.80 (s, 0.11H), 7.58 (s, 0.05H), 3.89 (s, 3H); **^{13}C NMR** (101 MHz, $CDCl_3$) δ (ppm) 163.7 (s), 142.9 (s), 139.3 (s), 129.8 (s), 127.0 (t, J = 25.5 Hz), 125.5 (t, J = 26.3 Hz), 53.4 (s); **MS** (ESI) *m/z* 178 [(M + Na)$^+$, 50], 156 [(M + H)$^+$, 50]; **HRMS** (ESI) *m/z* [M + H]$^+$ calculated for $C_7H_6D_2NO_3$ 156.0624, found 156.0619 (+2.2 ppm error).

Methyl 4,5-d_2-nicotinate S6

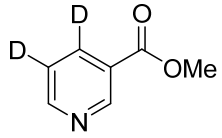

S6

To a solution of methyl 4,5-d_2-nicotinate *N*-oxide **S5** (240 mg, 1.36 mmol) and CH_2Cl_2 (8 mL) was added PCl_3 (0.8 mL) and the reaction heated to 40 °C for 2 h. The reaction was allowed to cool and quenched by careful addition onto ice. The resulting solution was adjusted to pH > 7 by addition of $NaHCO_{3(s)}$ and extracted with CH_2Cl_2 (3 × 50 mL). The combined extracts were concentrated under reduced pressure to afford the crude product. Purification by flash column chromatography (1:1 hexane-EtOAc) gave methyl 4,5-d_2-nicotinate **S6** (128 mg, 59%) as a pale yellow waxy solid, R_F (1:1 hexane-EtOAc) 0.3; **^{1}H NMR** (400 MHz, $CDCl_3$) δ (ppm) 9.24 (s, 1H), 8.79 (s, 1H), 8.30 (s, 0.11H), 7.40 (d, J = 4.1 Hz, 0.06 Hz), 3.97 (s, 3H); **^{13}C NMR** (101 MHz, $CDCl_3$) δ (ppm) 165.8 (s), 153.4 (s), 150.9 (S), 136.6 (t, J = 26.2 Hz), 125.9 (s), 122.9 (t, J = 25.8 Hz), 52.4 (s); **MS** (ESI) *m/z* 154 [$(M + H)^+$, 100]; **HRMS** (ESI) *m/z* $[M + H]^+$ calculated for $C_7H_6D_2NO_2$ 140.0675, found 140.0670 (+3.6 ppm error).

4,5-d_2-Nicotinamide 1c

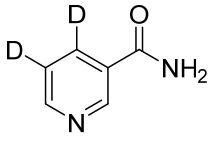

1c

Using General Procedure B, methyl-4,5-d_2-nicotinate **S6** (104 mg, 0.751 mmol) in ammonia (5 mL of a 7 N solution in MeOH) gave the crude product. Purification by reverse phase flash column chromatography (0-30% MeCN) gave 4,5-d_2-nicotinamide **1c** (62 mg, 67%) as a white solid, **^{1}H NMR** (400 MHz, d_6-DMSO) δ (ppm) 9.04 (s, 1H), 8.71 (s, 1H), 8.21 (s, 0.11H), 8.16 (br s, 1H), 7.60 (br s, 1H), 7.50 (d, J = 4.7 Hz, 0.06 Hz); **^{13}C NMR** (101 MHz, d_6-DMSO) δ (ppm) 166.9 (s), 152.3 (s), 149.1 (s), 135.2 (t, J = 25.2 Hz), 130.0 (s), 123.5 (t, J = 24.9 Hz); **MS** (ESI) *m/z* 147 [$(M + Na)^+$, 100], 125 [$(M + H)^+$, 83]; **HRMS** (ESI) *m/z* $[M + H]^+$ calculated for $C_6H_5D_2N_2O$ 125.0678, found 125.0677 (+1.0 ppm error).

Ethyl 5,6-d_2-nicotinate S7

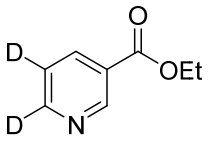

S7

Using General Procedure A, methyl 5,6-dichloronicotinate (160 mg, 0.776 mmol, 1.0 eq.), 5% Pd/C (30 mg, 20 wt%), K_2CO_3 (200 mg, 1.45 mmol, 1.9 eq.) and $D_{2(g)}$ (5 bar) in EtOD (10 mL) gave the crude product. Purification by flash column chromatography with 1:1 hexane-EtOAc as eluent gave ethyl 5,6-d_2-nicotinate **S7** (119 mg, 99%) as a pale yellow solid, R_F (1:1 hexane-EtOAc) 0.3; **^{1}H NMR** (400 MHz, $CDCl_3$) δ (ppm) 9.24 (d, J = 2.0 Hz, 1H), 8.31 (br. s, 1H), 4.43 (q, J = 7.1, 2H), 1.43 (t, J = 7.1 Hz, 3H); **^{13}C NMR** (101 MHz, $CDCl_3$) δ (ppm) 165.3 (s), 152.9 (t, J = 26.4 Hz), 150.9 (s), 136.9 (s), 126.3 (s), 122.8 (t, J = 24.7 Hz), 61.5 (s), 14.3 (s); **MS** (ESI) *m/z* 154 [$(M + H)^+$, 100], 126 [25]; **HRMS** (ESI) *m/z* $[M + H]^+$ calculated for C_8H_8-D_2NO_2 154.0832, found 154.0837 (–3.0 ppm error).

5,6-d_2-Nicotinamide 1d

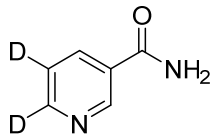

1d

Using General Procedure B, ethyl-5,6-d_2-nicotinate **S7** (119 mg, 0.776 mmol) in ammonia (5 mL of a 7 N solution in MeOH) gave the crude product. Purification by reverse phase flash column chromatography (0-30% MeCN) gave 5,6-d_2-nicotinamide **1d** (96 mg, 99%) as a white solid, **^{1}H NMR** (400 MHz, d_6-DMSO) δ (ppm) 9.04 (d, J = 2.3 Hz, 1H), 8.22 (d, J = 2.3 Hz, 1H), 8.19 (br s, 1H), 7.61 (br s, 1H); **^{13}C NMR** (101 MHz, d_6-DMSO) δ (ppm) 166.9 (s), 152.0 (t, J = 27.3 Hz), 149.1 (s), 135.5 (s), 130.1, 123.5 (t, J = 24.9 Hz); **MS** (ESI) *m/z* 147 [(M + Na)$^+$, 95], 125 [(M + H)$^+$, 100]; **HRMS** (ESI) *m/z* [M + H]$^+$ calculated for $C_6H_5D_2N_2O$ 125.0678, found 125.0679 (−0.3 ppm error).

5-Bromo-2-chloronicotinamide S8

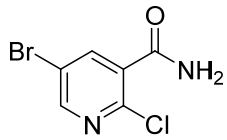

S8

A solution of methyl 5-bromo-2-chloronicotinate (250 mg, 1 mmol) was dissolved in ammonia (5 mL of a 7 N solution in MeOH) and the resulting solution stirred at rt for 16 h. Concentration under reduced pressure afforded 5-bromo-2-chloronicotinamide **S8** (235 mg, 100%) as a crystalline white solid, used without further purification. **^{1}H NMR** (500 MHz, d_6-DMSO) δ (ppm) 8.64 (s, 1H), 8.22 (s, 1H), 8.12 (br. S, 1H), 7.88 (br.s, 1H); **^{13}C NMR** (126 MHz, d_6-DMSO) δ (ppm) 165.8 (s), 151.0 (s), 145.8 (s), 140.4 (s), 135.0 (s), 119.3 (s); **MS** (ESI) *m/z* 239 [(^{81}Br /^{37}Cl-M + H)$^+$, 30] , 237 [(^{81}Br /^{35}Cl-M + H)$^+$, (^{79}Br /^{37}Cl-M + H)$^+$, 100], 235 [(^{79}Br /^{35}Cl-M + H)$^+$,80].

Methyl-2,5-d_2-nicotinate 1e

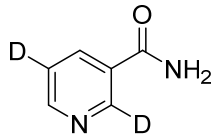

1e

Using General Procedure A, 5-bromo-2-chloronicotinamide **S8** (100 mg, 0.425 mmol, 1.0 eq.), 5% Pd/C (20 mg, 20 wt%), K_2CO_3 (150 mg, 1.09 mmol, 2.5 eq.) and $D_{2(g)}$ (7 bar) in EtOD (10 mL) gave the crude product. Purification by reverse phase flash column chromatography (0-30% MeCN) gave 2,5-d_2-nicotinamide **1e** (46 mg, 87%) as a white solid, **^{1}H NMR** (400 MHz, d_6-DMSO) δ (ppm) 8.7 (d, J = 1.5 Hz, 1H), 8.21 (d, J = 1.5 Hz, 1H), 8.19 (br s, 1H), 7.61 (br s, 1H); **^{13}C NMR** (101 MHz, d_6-DMSO) δ (ppm) 166.9 (s), 152.3 (s), 148.8 (t, J =

26.9 Hz), 135.5 (s), 130.0 (s), 123.6 (t, *J* = 23.1 Hz); **MS** (ESI) *m/z* 125 [(M + H)$^+$, 100]; **HRMS** (ESI) *m/z* [M + H]$^+$ calculated for $C_6H_5D_2N_2O$ 125.0678, found 125.0685 (−4.9 ppm error).

Methyl 4,6-*d*$_2$-nicotinate 2b

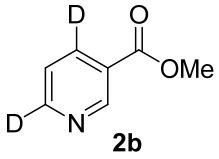

2b

5% Pd/C (50 mg, 10 wt%) was added to a stirred suspension of 4,6-dichloronicotinic acid (500 mg, 2.63 mmol, 1.0 eq.) and K_2CO_3 (910 mg, 6.58 mmol, 2.5 eq.) in a 1:1 mix of THF-D_2O (14 mL) in a 30 mL Parr Reactor. The Parr reactor was sealed, purged with $N_{2(g)}$ and pressurised with $D_{2(g)}$ (8 bar). The reaction was stirred at rt for 16h. Then, the pressure was released and the suspension was filtered through Celite® and washed with CH_2Cl_2 (3 x 15 mL). The filtrate was concentrated under reduced pressure to give a solid residue that was dissolved in CH_2Cl_2 (10 mL). Then, oxalyl chloride (265 µL, 3.16 mmol, 1.2 eq.) and DMF (2 drops) were added and the resulting solution was stirred at rt for 1 h. The reaction was concentrated under reduced pressure and CH_2Cl_2 (10 mL), Et_3N (857 µL, 6.58 mmol, 2.5 eq.) and MeOH (1.0 mL) were added sequentially. The resulting solution was stirred at rt for 10 min. The aqueous layer was extracted with CH_2Cl_2 (2 x 10 mL). The combined organic layers were dried ($MgSO_4$) and concentrated under reduced pressure to give the crude product. Purification by flash column chromatography with 1:1 petrol-EtOAc as eluent gave methyl-4,6-*d*$_2$-nicotinate **2b** (318 mg, 78%) as a pale yellow solid, R_F (1:1 petrol-EtOAc) 0.3; **^{1}H NMR** (400 MHz, $CDCl_3$) δ (ppm) 9.18 (s, 1H), 7.36 (s, 1H), 3.92 (s, 3H); **^{13}C NMR** (101 MHz, $CDCl_3$) δ (ppm) 165.7 (s), 153.0 (t, *J* = 27.4 Hz), 150.8 (s), 136.8 (t, *J* = 25.4 Hz), 125.9 (s), 123.0 (s), 52.4 (s); **MS** (ESI) *m/z* 140 [(M + H)$^+$, 100]; **HRMS** (ESI) *m/z* [M + H]$^+$ calculated for $C_7H_6D_2NO_2$ 140.0675, found 140.0673 (+1.5 ppm error).

4,6-*d*$_2$-Nicotinamide 1f

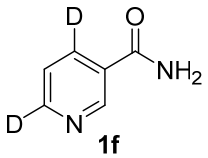

1f

Using General Procedure B, methyl-4,6-*d*$_2$-nicotinate **2b** (200 mg, 1.31 mmol) in ammonia (10 mL of a 7 N solution in MeOH) gave the crude product. Purification by reverse phase flash column chromatography (0-30% MeCN) gave 4,6-*d*$_2$-nicotinamide **1f** (144 mg, 89%) as a white solid, **^{1}H NMR** (400 MHz, d_6-DMSO) δ (ppm) 9.03 (s, 1H), 8.19 (br s, 1H), 7.63 (br s, 1H), 7.50 (s, 1H); **^{13}C NMR** (101 MHz, d_6-DMSO) δ (ppm) 166.9 (s), 152.0 (t, *J* = 27.5 Hz), 149.1 (s), 135.3 (t, *J* = 24.9 Hz), 130.0 (s), 123.6 (s); **MS** (ESI) *m/z* 147 [(M + Na)$^+$, 55], 125 [(M + H)$^+$, 100]; **HRMS** (ESI) *m/z* [M + H]$^+$ calculated for $C_6H_5D_2N_2O$ 125.0678, found 125.0681 (−1.8 ppm error).

Ethyl 4,5,6-d_3-nicotinate S9

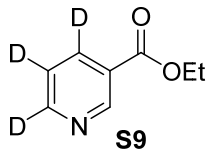

S9

Using General Procedure A, ethyl-4,5,6-trichloronicotinate(2) (150 mg, 0.60 mmol, 1.0 eq.), 5% Pd/C (15 mg, 10 wt%), K_2CO_3 (207 mg, 2.10 mmol, 3.5 eq.) and $D_{2(g)}$ (5 bar) in EtOD (10 mL) gave the crude product. Purification by flash column chromatography with 1:1 petrol-EtOAc as eluent gave ethyl-4,5,6-d_3-nicotinate **S9** (68 mg, 75%) as a pale yellow solid, R_F (1:1 petrol-EtOAc) 0.3; **^{1}H NMR** (400 MHz, $CDCl_3$) δ (ppm) 9.24 (s, 1H), 4.41 (q, J = 8.0 Hz, 2H), 1.43 (t, J = 8.0 Hz, 3H); **^{13}C NMR** (101 MHz, $CDCl_3$) δ (ppm) 165.3 (s), 152.9 (t, J = 26.6 Hz), 150.9 (s), 136.6 (t, J = 25.4 Hz), 126.3 (s), 122.7 (t, J = 25.4 Hz), 61.4 (s), 14.3 (s); **MS** (ESI) *m/z* 177 [$(M + Na)^+$, 100], 155 [$(M + H)^+$, 50]; **HRMS** (ESI) *m/z* $[M + H]^+$ calculated for $C_8H_6D_3NO_2$ 177.0719, found 177.0719 (−0.1 ppm error).

4,5,6-d_3-Nicotinamide 1g

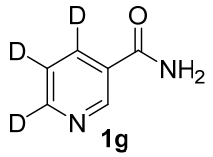

1g

Using General Procedure B, ethyl-4,5,6-d_3-nicotinate **S9** (60 mg, 0.39 mmol) in ammonia (10 mL of a 7 N solution in MeOH) gave the crude product. Purification by reverse phase flash column chromatography (0-30% MeCN) gave 4,5,6-d_3-nicotinamide **1g (**39 mg, 94%) as a white solid, **^{1}H NMR** (400 MHz, d_6-DMSO) δ (ppm) 9.04 (s, 1H), 8.17 (br s, 1H), 7.60 (br s, 1H); **^{13}C NMR** (101 MHz, d_6-DMSO) δ (ppm) 166.9 (s), 152.0 (t, J = 27.7 Hz), 149.2 (s), 135.2 (t, J = 25.6 Hz), 130.0 (s), 123.3 (t, J = 25.6 Hz); **MS** (ESI) *m/z* 148 [$(M + Na)^+$, 50], 126 [$(M + H)^+$, 100]; **HRMS** (ESI) *m/z* $[M + H]^+$ calculated for $C_6H_4D_3N_2O$ 126.0741, found 126.0744 (−1.9 ppm error).

d_3-Methyl nicotinate 2a

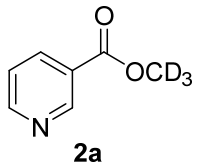

2a

CD_3OD (2.0 mL) was added to a stirred solution of nicotinoyl chloride hydrochloride (534 mg, 3.0 mmol, 1.0 eq.) and Et_3N (1.04 mL, 7.5 mmol, 2.5 eq.) in CH_2Cl_2 (10 mL) at rt under N_2. The resulting solution was stirred at rt for 10 min. Then, a saturated solution of $NaHCO_3$(aq) (20 mL) was added and the two layers were separated. The aqueous layer was extracted with CH_2Cl_2 (2 x 10 mL). The combined organic layers were dried ($MgSO_4$) and concentrated under reduced pressure to give the crude product. Purification by flash

column chromatography with 1:1 petrol-EtOAc as eluent gave d_3-methyl nicotinate **2a** (320 mg, 78%) as a pale yellow solid, R_F (1:1 petrol-EtOAc) 0.3; **^{1}H NMR** (400 MHz, $CDCl_3$) δ (ppm) 9.18 (dd, J = 2.1, 0.8 Hz, 1H), 8.73 (dd, J = 4.9, 1.7 Hz, 1H), (ddd, J = 7.9, 2.1, 1.7 Hz, 1H), 7.35 (ddd, J = 7.9, 4.9, 0.8 Hz, 1H); **^{13}C NMR** (101 MHz, $CDCl_3$) δ (ppm) 165.7 (s), 153.4 (s), 150.9 (s), 137.0 (s), 126.0 (s), 123.2 (s), 51.6 (sept., J = 22.5 Hz); **MS** (ESI) m/z 141 [$(M + H)^+$, 100]; **HRMS** (ESI) m/z [M + H]$^+$ calculated for $C_7H_5D_3NO_2$ 141.0738, found 141.0736 (+1.2 ppm error).

d_3-Methyl-4,6-d_2-nicotinate 2c

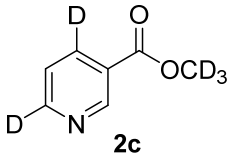

2c

5% Pd/C (50 mg, 10 wt%) was added to a stirred suspension of 4,6-dichloronicotinic acid (500 mg, 2.63 mmol, 1.0 eq.) and K_2CO_3 (910 mg, 6.58 mmol, 2.5 eq.) in a 1:1 mix of THF-D_2O (14 mL) in a 30 mL Parr Reactor. The Parr reactor was sealed, purged with $N_{2(g)}$ and pressurised with $D_{2(g)}$ (8 bar). The reaction was stirred at rt for 16h. Then, the pressure was released and the suspension was filtered through Celite® and washed with CH_2Cl_2 (3 x 15 mL). The filtrate was concentrated under reduced pressure to give a solid residue that was dissolved in CH_2Cl_2 (10 mL). Then, oxaloyl chloride (265 µL, 3.16 mmol, 1.2 eq.) and DMF (2 drops) were added and the resulting solution was stirred at rt for 1 h. The reaction was concentrated under reduced pressure and CH_2Cl_2 (10 mL), Et_3N (857 µL, 6.58 mmol, 2.5 eq.) and CD_3OD (1.0 mL) were added sequentially. The resulting solution was stirred at rt for 10 min. The aqueous layer was extracted with CH_2Cl_2 (2 x 10 mL). The combined organic layers were dried ($MgSO_4$) and concentrated under reduced pressure to give the crude product. Purification by flash column chromatography with 1:1 petrol-EtOAc as eluent gave d_3-methyl-4,6-d_2-nicotinate **2a** (333 mg, 91%) as a pale yellow solid, R_F (1:1 petrol-EtOAc) 0.3; **^{1}H NMR** (400 MHz, $CDCl_3$) δ (ppm) 9.16 (s, 1H), 7.34 (s, 1H); **^{13}C NMR** (101 MHz, $CDCl_3$) δ (ppm) 165.7 (s), 153.0 (t, J = 27.4 Hz), 150.8 (s), 136.7 (t, J = 25.4 Hz), 125.9 (s), 123.0 (s), 51.6 (sept., J = 22.6 Hz); **MS** (ESI) m/z 143 [$(M + H)^+$, 100]; **HRMS** (ESI) m/z [M + H]$^+$ calculated for $C_7H_3D_5NO_2$ 143.0863, found 143.0858 (+3.2 ppm error).

Methyl-2,4-d_2-nicotinate 2d

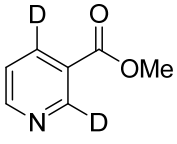

2d

5% Pd/C (50 mg, 10 wt%) was added to a stirred suspension of 2,5-dichloronicotinic acid (500 mg, 2.63 mmol, 1.0 eq.) and K_2CO_3 (910 mg, 6.58 mmol, 2.5 eq.) in a 1:1 mix of THF-D_2O (14 mL) in a 30 mL Parr Reactor. The Parr reactor was sealed, purged with $N_{2(g)}$ and pressurised with $D_{2(g)}$ (8 bar). The reaction was stirred at rt for 16h. Then, the pressure was released and the suspension was filtered through Celite® and washed with CH_2Cl_2 (3 x 15

mL). The filtrate was concentrated under reduced pressure to give a solid residue that was dissolved in CH_2Cl_2 (10 mL). Then, oxalyl chloride (265 µL, 3.16 mmol, 1.2 eq.) and DMF (2 drops) were added and the resulting solution was stirred at rt for 1 h. The reaction was concentrated under reduced pressure and CH_2Cl_2 (10 mL), Et_3N (857 µL, 6.58 mmol, 2.5 eq.) and MeOH (1.0 mL) were added sequentially. The resulting solution was stirred at rt for 10 min. The aqueous layer was extracted with CH_2Cl_2 (2 x 10 mL). The combined organic layers were dried ($MgSO_4$) and concentrated under reduced pressure to give the crude product. Purification by flash column chromatography with 1:1 petrol-EtOAc as eluent gave methyl-2,5-d_2-nicotinate **2d** (293 mg,72%) as a pale yellow solid, R_F (1:1 petrol-EtOAc) 0.3; **^{1}H NMR** (400 MHz, $CDCl_3$) δ (ppm) 8.79 (s, 1H), 8.31 (s, 1H), 3.97 (s, 3H); **^{13}C NMR** (101 MHz, $CDCl_3$) δ (ppm) 165.8 (s), 153.4 (s), 150.6 (t, J = 28.1 Hz), 137.0 (s), 125.9 (s), 123.0 (t, J = 25.4 Hz), 52.44 (s); **MS** (ESI) *m/z* 140 [(M + H)$^+$, 100]; **HRMS** (ESI) *m/z* [M + H]$^+$ calculated for $C_7H_6D_2NO_2$ 140.0675, found 140.0681 (−4.8 ppm error).

Methyl-2,5-d_2-nicotinate 2e

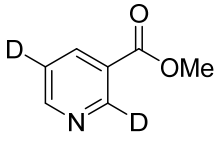

2e

5% Pd/C (50 mg, 10 wt%) was added to a stirred suspension of 2,5-dichloronicotinic acid (500 mg, 2.63 mmol, 1.0 eq.) and K_2CO_3 (910 mg, 6.58 mmol, 2.5 eq.) in a 1:1 mix of THF-D_2O (14 mL) in a 30 mL Parr Reactor. The Parr reactor was sealed, purged with $N_{2(g)}$ and pressurised with $D_{2(g)}$ (8 bar). The reaction was stirred at rt for 16h. Then, the pressure was released and the suspension was filtered through Celite® and washed with CH_2Cl_2 (3 x 15 mL). The filtrate was concentrated under reduced pressure to give a solid residue that was dissolved in CH_2Cl_2 (10 mL). Then, oxalyl chloride (265 µL, 3.16 mmol, 1.2 eq.) and DMF (2 drops) were added and the resulting solution was stirred at rt for 1 h. The reaction was concentrated under reduced pressure and CH_2Cl_2 (10 mL), Et_3N (857 µL, 6.58 mmol, 2.5 eq.) and MeOH (1.0 mL) were added sequentially. The resulting solution was stirred at rt for 10 min. The aqueous layer was extracted with CH_2Cl_2 (2 x 10 mL). The combined organic layers were dried ($MgSO_4$) and concentrated under reduced pressure to give the crude product. Purification by flash column chromatography with 1:1 petrol-EtOAc as eluent gave methyl-2,5-d_2-nicotinate **2e** (253 mg, 62%) as a pale yellow solid, R_F (1:1 petrol-EtOAc) 0.3; **^{1}H NMR** (400 MHz, $CDCl_3$) δ (ppm) 8.79 (s, 1H), 8.31 (s, 1H), 3.97 (s, 3H); **^{13}C NMR** (101 MHz, $CDCl_3$) δ (ppm) 165.8 (s), 153.4 (s), 150.6 (t, J = 28.1 Hz), 137.0 (s), 125.9 (s), 123.0 (t, J = 25.4 Hz), 52.44 (s); **MS** (ESI) *m/z* 140 [(M + H)$^+$, 100]; **HRMS** (ESI) *m/z* [M + H]$^+$ calculated for $C_7H_6D_2NO_2$ 140.0675, found 140.0677 (−1.8 ppm error).

Methyl 2,4,5,6-d_4-nicotinate

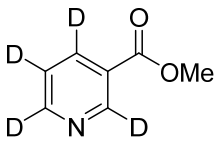

A solution of 3-bromo-2,4,5,6-d_4-pyridine *N*-oxide **S3** (1.00 g, 6.17 mmol), K_2CO_3 (1.10 g, 8.02 mmol, 1.3eq.), $PdCl_2$(dppf) (244 mg, 0.31 mmol,5 mol%) and MeOH (30 mL) was heated to 75 °C under $CO_{(g)}$ (4 Bar) for 4 h. The reaction was allowed to cool and concentrated under reduced pressure to afford the crude product. The residue was dissolved in CH_2Cl_2 (30 mL) and PCl_3 (2.0 mL) was added. Then, the reaction was heated to 40 °C for 2 h. The reaction was allowed to cool and quenched by careful addition onto ice. The resulting solution was adjusted to pH > 7 by addition of $NaHCO_{3(s)}$ and extracted with CH_2Cl_2 (3 × 50 mL). The combined extracts were concentrated under reduced pressure to afford the crude product. Purification by flash column chromatography (1:1 hexane-EtOAc) gave methyl 2,4,5,6-d_4-nicotinate (644 mg, 74%) as a pale yellow solid, R_F (1:1 hexane-EtOAc) 0.3; **^{1}H NMR** (400 MHz, $CDCl_3$) δ (ppm) 3.95 (s, 3H); **^{13}C NMR** (101 MHz, $CDCl_3$) δ (ppm) 165.7 (s), 153.0(t, *J* = 27.0 Hz), 150.6 (t, *J* = 28.5 Hz), 136.6 (t, *J* = 26.0 Hz), 125.8 (s), 122.8 (t, *J* = 24.7 Hz), 52.4 (s); **MS** (ESI) *m/z* 142 [(M + H)$^+$, 100]; **HRMS** (ESI) *m/z* [M + H]$^+$ calculated for $C_7H_3D_4NO_2$ 142.0806, found 142.0808 (+1.6 ppm error).

***d*$_{11}$-2,4,6-trimethylaniline**

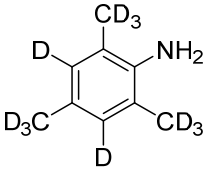

Acetic acid (1.80 mL) was added dropwise to a stirred solution of d_{11}-nitromesitylene (783 mg, 4.45 mmol, 1.0 eq.) and zinc powder (1.47 g, 22.25 mmol, 5.0 eq.) in EtOH (15 mL) at 0 °C. The resulting solution was warmed to rt and stirred at rt for 5 h. Then, 1 M NaOH(aq) (10 mL) was added and the mixture was extracted with hexane (3 x 15 mL). The combined organic layers were dried ($MgSO_4$) and concentrated under reduced pressure to give *d*$_{11}$-2,4,6-trimethylaniline (583 mg, 90 %) as an orange oil, **^{1}H NMR** (400 MHz, $CDCl_3$) δ 3.37 (br s, 2H, NH_2); **^{13}C NMR** (100.6 MHz, $CDCl_3$) δ 140.0 (CNH_2), 128.7 (t, *J* = 22 Hz, CD), 126.9 (s), 121.7 (s), 19.4 (sept., *J* = 20 Hz, CD_3), 16.7 (sept, *J* = 20 Hz, CD_3); **MS** (ESI) m/z 147 [(M + H)$^+$, 100]; **HRMS** m/z [M + H]$^+$ calcd for $C_9H_3D_{11}N$ 147.1817, found 147.1819 (+0.3 ppm error). Spectroscopic data consistent with those reported in the literature.(4)

***d*$_{22}$-2,4,6-Trimethyl-*N* -[2-[(2,4,6-trimethylphenyl)imino]ethylidene]aniline**

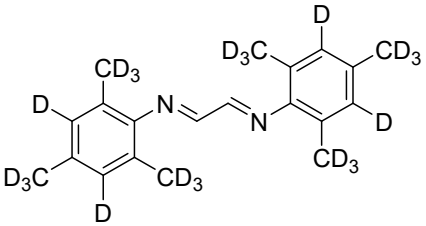

Glyoxal (160 µL of a 40 w/w% in H_2O, 1.37 mmol, 1.0 eq.) and formic acid (2 drops) were added sequentially to a stirred solution of d_{11}-mesitylaniline (400 mg, 2.74 mmol, 2.0 eq.) in MeOH at rt. The resulting solution was stirred at rt for 16 h during which time a yellow precipitate formed. The precipitate was filtered, washed with MeOH and dried under vacuum to give the ethylenediimine (293 mg, 68%) as a yellow crystalline solid, **^{1}H NMR** (400 MHz, $CDCl_3$) δ 8.12 (s, 2H); **^{13}C NMR** (100.6 MHz, $CDCl_3$) δ 163.4 (s), 147.5 (s), 134.0 (s), 128.7 (t, *J* = 22 Hz, CD), 126.4 (s), 19.9 (sept., *J* = 20 Hz, CD_3), 17.3 (sept, *J* = 20 Hz, CD_3); **MS**

(ESI) m/z 337 [(M + Na)$^+$, 30], 315 [(M + H)$^+$, 100]; **HRMS** m/z [M + H]$^+$ calcd for $C_{20}H_3D_{22}N_2$ 315.3393, found 315.3378 (+4.7 ppm error).

d_{22}-1,3-Bis-(2,4,6-trimethylphenyl)imidazolium chloride (d_{22}-IMes.HCl)

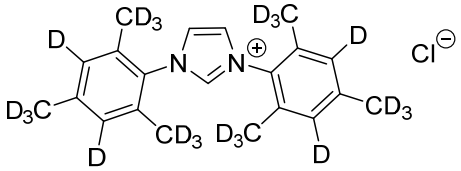

A solution of paraformaldehyde (32 mg, 1.05 mmol, 1.1 eq.) in 4 M $HCl_{(dioxane)}$ (0.36 mL, 1.43 mmol, 1.5 eq.) was added dropwise to a stirred solution of the diimine (300 mg, 0.95 mmol, 1.0 eq.) in EtOAc (10 mL) at rt under N_2. The resulting solution was stirred at rt for 16 h during which time an off white precipitate formed. Then, the precipitate was filtered, washed with EtOAc and dried under vacuum to give d_{22}-IMes.HCl (291 mg, 81%) as a white powder, **^{1}H NMR** (400 MHz, $CDCl_3$) δ 10.21 (br s, 1H, NCH), 7.66 (s, 2H, CH); **^{13}C NMR** (100.6 MHz, $CDCl_3$) δ 141.0 (s), 139.4 (s), 133.9 (s), 130.7 (s), 129.6 (t, J = 24 Hz, CD), 124.6 (s), 20.2 (sept., J = 19 Hz, CD_3), 16.8 (sept, J = 19 Hz, CD_3); **MS** (ESI) m/z 327 [(M − Cl)$^+$, 100]; **HRMS** m/z calcd for $C_{21}H_3D_{22}N_2$ (M − Cl)$^+$ 327.3393, found 327.3376 (+4.8 ppm error).

d_3-1,3-Bis-(2,4,6-trimethylphenyl)imidazolium chloride (d_3-IMes.HCl)

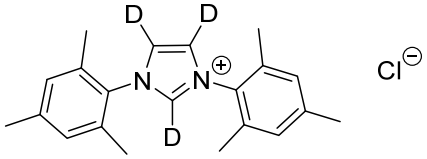

K_2CO_3 (21 mg, 0.15 mmol, 0.05 eq.) was added to a stirred solution of IMes.HCl (1.02 g, 3.00 mmol, 1.0 eq.) in D_2O (6 mL) at rt. The resulting solution was heated at 100 °C for 16 h. Then, solvent was removed under reduced pressure to give the crude product. The solid was washed with EtOAc to give d_3-IMes.HCl (1.00 g, 97%, 96% deuterium incorporation by ^{1}H NMR spectroscopy) as a white powder, **^{1}H NMR** (400 MHz, $CDCl_3$) δ 7.02 (s, 4H), 2.34 (s, 6H), 2.18 (s, 12H); **^{13}C NMR** (100.6 MHz, $CDCl_3$) δ 141.4 (s), 134.1 (s), 130.6 (s), 130.0 (s), 130.5 (s), 129.9 (s), 124.2 (t, J = 25 Hz, CD), 21.2 (s), 17.7(s); **MS** (ESI) m/z 308 [(M)$^+$, 100]; **HRMS** m/z calcd for $C_{21}H_{23}D_3N_2$ (M)$^+$ 308.2206, found 308.2213 (−2.3 ppm error). Contains *ca.* 4% IMes.HCl as characterised by ^{1}H NMR (400 MHz, $CDCl_3$) δ 10.82 (s, 0.04H, NCH), 7.64 (s, 0.04H).

d_{25}-1,3-Bis-(2,4,6-trimethylphenyl)imidazolium chloride (d_{25}-IMes.HCl)

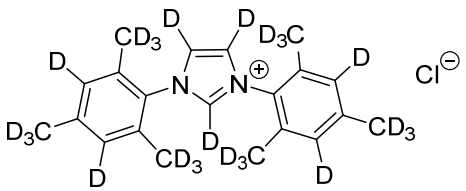

K_2CO_3 (10 mg, 0.07 mmol, 0.05 eq.) was added to a stirred solution of d_{22}-IMes.HCl(5) (500 mg, 1.38 mmol, 1.0 eq.) in D_2O (10 mL) at rt. The resulting solution was heated at 100 °C for 16 h. Then, solvent was removed under reduced pressure to give the crude product. The solid was washed with EtOAc to give d_{25}-IMes.HCl (490 mg, 97%) as a white powder, **^{13}C NMR** (100.6 MHz, $CDCl_3$) δ 141.1 (s), 139.5 (t, J = 18 Hz , CD), 133.9 (s), 130.7 (s), 129.6 (t, J =

27 Hz, CD), 124.4 ((t, *J* = 29 Hz, CD), 20.2 (sept., *J* = 29 Hz, CD_3) 16.8 (sept., *J* = 29 Hz, CD_3); **MS** (ESI) m/z 330 [(M− Cl)$^+$, 100]; **HRMS** m/z calcd for $C_{21}D_{25}N_2$ (M − Cl)$^+$ 330.3587, found 330.3590 (+3.1 ppm error).

[IrCl(COD)(*d*$_2$-IMes)]

KO^{t}Bu (62 mg, 0.55 mmol, 2.4eq.) was added to a stirred solution of d_3-IMes.HCl (172 mg, 0.50 mmol, 2.2 eq.) in THF at rt under N_2. The resulting suspension was stirred at rt for 30 min. Then, a solution of $[Ir(COD)Cl]_2$ (154 mg, 0.23 mmol, 1.0 eq.) was added and the resulting solution was stirred at rt for 2 h. The solvent was removed under reduced pressure to give the crude product. Purification by flash column chromatography on silica with CH_2Cl_2 as eluent gave [IrCl(COD)(d_2-IMes)] (112 mg, 76%) as a yellow crystalline solid, R_f (CH_2Cl_2) 0.2; **^{1}H NMR** (400 MHz, $CDCl_3$) δ 7.04 (s, 2H), 7.01 (s, 2H), 4.21-4.16 (m, 2H), 3.03-2.99 (m, 2H), 2.39 (br s, 12H), 2.19 (s, 6H), 1.79-1.65 (m, 4H), 1.41-1.28 (m, 4H); **^{13}C NMR** (100.6 MHz, $CDCl_3$) δ 180.7 (s), 138.6 (s), 137.3 (s), 136.0 (s), 134.4 (s), 129.5 (s), 128.1 (s), 123.2 (t, *J* = 18 Hz, CD), 82.6 (s), 51.5 (s), 33.5 (s), 28.9 (s), 21.2 (s), 19.7 (s), 18.2 (s); **MS** (ESI, CH_3CN) m/z 607 [(M(^{193}Ir) – Cl)$^+$, 40], 605 [(M(^{191}Ir) – Cl)$^+$, 20]; **HRMS** in CH_3CN m/z calcd for $C_{29}H_{34}D_2{}^{193}IrN_2$ (M – Cl)$^+$ 607.2633, found 607.2638 (−3.8 ppm error).

[IrCl(COD)(*d*$_{22}$-IMes)]

KO^{t}Bu (27 mg, 0.24 mmol, 2.4eq.) was added to a stirred solution of d_{22}-IMes.HCl (75 mg, 0.22 mmol, 2.2 eq.) in THF at rt under N_2. The resulting suspension was stirred at rt for 30 min. Then, a solution of $[Ir(COD)Cl]_2$ (67 mg, 0.10 mmol, 1.0 eq.) was added and the resulting solution was stirred at rt for 2 h. The solvent was removed under reduced pressure to give the crude product. Purification by flash column chromatography on silica with CH_2Cl_2 gave [IrCl(COD)(d_{22}-IMes)] (78 mg, 56%) as a yellow crystalline solid, R_f (CH_2Cl_2) 0.2; **^{1}H NMR** (400 MHz, $CDCl_3$) δ 6.88 (s, 2H), 4.10-4.05 (m, 2H), 2.91-2.88 (m, 2H), 1.66-1.51 (m, 4H), 1.30-1.12 (m, 4H); **^{13}C NMR** (100.6 MHz, $CDCl_3$) δ 180.7 (s), 138.4 (s), 137.1 (s), 136.1 (s), 134.2 (s), 129.3 (t, *J* = 23 Hz, CD), 127.9 (t, *J* = 24 Hz, CD),, 123.3 (s), 82.5 (s), 51.4 (s), 33.5 (s), 29.0 (s), 20.3(sept., *J* = 22 Hz, CD_3), 18.8 (sept., *J* = 20 Hz, CD_3), 17.6 (sept., *J* = 22 Hz, CD_3); **MS** (ESI, CH_3CN) m/z 668 [(M(^{193}Ir) – Cl + CH_3CN)$^+$, 100], 666 [(M(^{191}Ir) – Cl + CH_3CN)$^+$, 60], 627 [(M(^{193}Ir) – Cl)$^+$, 50], 625 [(M(^{191}Ir) – Cl)$^+$, 30]; **HRMS** in CH_3CN m/z calcd for $C_{31}H_{17}D_{22}{}^{193}IrN_3$ (M – Cl + CH_3CN)$^+$ 668.4164, found 668.4172 (+5.0 ppm error).

[IrCl(COD)(*d*$_{24}$-IMes)]

KO^{t}Bu (62 mg, 0.55 mmol, 2.4eq.) was added to a stirred solution of d_{25}-IMes.HCl (183 mg, 0.50 mmol, 2.2 eq.) in THF at rt under N_2. The resulting suspension was stirred at rt for 30 min. Then, a solution of $[Ir(COD)Cl]_2$ (154 mg, 0.23 mmol, 1.0 eq.) was added and the resulting solution was stirred at rt for 2 h. The solvent was removed under reduced pressure to give the crude product. Purification by flash column chromatography on silica with CH_2Cl_2 as eluent gave [IrCl(COD)(d_{24}-IMes)] (124 mg, 81%) as a yellow crystalline solid, R_f (CH_2Cl_2) 0.2; **^{1}H NMR** (400 MHz, $CDCl_3$) δ 4.19-4.17 (m, 2H), 3.01-2.99 (m, 2H), 1.75-1.68 (m, 4H), 1.40-1.23 (m, 4H); **^{13}C NMR** (100.6 MHz, $CDCl_3$) δ 180.6 (s), 138.4 (s), 137.1 (s), 136.1 (s), 134.2 (s), 129.3 (t, *J* = 22 Hz, CD), 127.8 (t, *J* = 25 Hz, CD), 123.0 (t, *J* = 26 Hz), 82.5 (s), 77.3 (s), 51.4 (s), 33.5 (s), 29.0 (s), 20.4 (sept., *J* = 20 Hz, CD_3), 18.8 (sept., *J* = 20 Hz, CD_3), 17.4 (sept., *J* = 21 Hz, CD_3); **MS** (ESI) m/z 629 [(M(^{193}Ir) – Cl)$^+$, 40], 627 [(M(^{191}Ir) – Cl)$^+$, 20]; **HRMS** m/z calcd for $C_{29}H_{12}D_{24}{}^{193}IrN_2$ (M – Cl)$^+$ 629.4010, found 629.4000 (+4.9 ppm error).

Contains *ca.* 10% [IrCl(COD)(d_{22}-IMes)] as characterised by ^{1}H NMR (400 MHz, $CDCl_3$) δ 6.99 (s, 0.20H).

3,5-d_2-pyridazine 3a

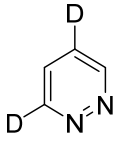

3a

Using general procedure A, 3,5-dichloropyridazine (1.0 g, 6.7 mmol, 1.0 eq.), K_2CO_3 (2.8 g, 20 mmol, 3 eq.), 5% Pd/C (50 mg, 10 wt%) and D_2 (8 bar). in THF (5 mL) and D_2O (5 mL) gave the crude product. Purification by flash column chromatography with EtOAc as eluent to give 3,5-d_2-pyridazine **3a** (240 mg, 44%) as a light yellow oil; **^{1}H NMR** (400 MHz, $CDCl_3$) δ 9.07 (s, 1H), 7.38 (s, 1H); **^{13}C NMR** (101 MHz, $CDCl_3$) δ 151.5 (s), 151.2 (t, J = 28.0 Hz), 126.1 (s), 126.0 (t, J = 25.8 Hz); **MS** (ESI) *m/z* 83 [(M + H)$^+$, 100]; **HRMS** (ESI) *m/z* [M + H]$^+$ calculated for $C_4H_3D_2N_2$ 83.0573, found 83.0575 (–3.6 ppm error).

2,5-d_2-pyrimidine 4a

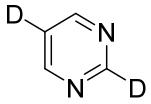

4a

To a suspension of 2,5-dichloropyrimidine (500 mg, 3.4 mmol, 1.0 eq.) and K_2CO_3 (1.4 g, 10 mmol, 3 eq.) in THF (5 mL) and D_2O (5 mL) in a 30 mL Parr reactor was added 5% Pd/C (50 mg, 10 wt%). The reactor was sealed, purged with N_2, then pressurised with D_2 (8 bar). The reaction mixture was stirred at room temperature for 1 hour. The pressure was released and the suspension was filtered through Celite® and washed with diethyl ether (20 mL). The filtrate was washed with brine (20 mL), dried over $MgSO_4$ then acidified with HCl (2 M in diethyl ether, 2 mL). The resulting suspension was decanted to leave an oily residue which solidified under a stream of nitrogen. This solid was dissolved in methanol-d_4 (4 mL) and passed through a plug of basic alumina to give a solution of 2,5-d_2-pyrimidine **4a** (0.565 M in methanol-d_4), **^{1}H NMR** (400 MHz, MeOD) δ 8.81 (s, 2H); **^{13}C NMR** (101 MHz, MeOD) δ 158.8 (t, J = 31.2 Hz), 158.3 (s), 123.2 (t, J = 26.1 Hz); **MS** (ESI) *m/z* 83 [(M + H)$^+$, 100]. The concentration was determined by quantitative ^{1}H NMR with potassium phthalate monobasic as an internal standard.

2,5-d_2-pyrazine 5a

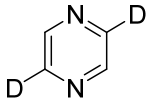

5a

To a suspension of 2,5-dichloropyrazine (500 mg, 3.4 mmol, 1.0 eq.) and K_2CO_3 (925 mg, 6.7 mmol, 2 eq.) in THF (5 mL) and D_2O (5 mL) in a 30 mL Parr reactor was added 5% Pd/C (50 mg, 10 wt%). The reactor was sealed, purged with N_2, then pressurised with D_2 (8 bar). The reaction mixture was stirred at room temperature for 1 hour. The pressure was released

and the suspension was filtered through Celite® and washed with diethyl ether (20 mL). The filtrate was washed with brine (20 mL), dried over $MgSO_4$ then acidified with HCl (2 M in diethyl ether, 2 mL). The resulting suspension was decanted to leave an oily residue which solidified under a stream of nitrogen. This solid was dissolved in methanol-d_4 (4 mL) and passed through a plug of basic alumina to give a solution of 2,5-d_2-pyrazine **5a** (0.088 M in methanol-d_4); **^{1}H NMR** (400 MHz, MeOD) δ 8.64 (s, 2H); **^{13}C NMR** (101 MHz, MeOD) δ 146.1 (s), 145.9 (t, J = 28.2 Hz); **MS** (ESI) m/z 83 [$(M + H)^+$, 100]. The concentration was determined by quantitative ^{1}H NMR with potassium phthalate monobasic as an internal standard.

Methyl 2,5-dichloroisonicotinate S9

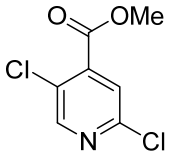

S9

To a solution of 2,5-dichloroisonicotinic acid (500 mg, 2.6 mmol, 1.0 eq.) in methanol (5 mL) and diethyl ether (5 mL) was added (trimethylsilyl)diazomethane solution (2.6 mL, 2.0 M in diethyl ether, 2 eq.). The reaction mixture was stirred at room temperature for 30 minutes, then concentrated under reduced pressure and purified by flash column chromatography with 4:1 petrol-EtOAc as eluent to give methyl 2,5-dichloroisonicotinate **S9** (518 mg, 97%) as a colourless solid, **^{1}H NMR** (400 MHz, $CDCl_3$) δ 8.43 (s, 1H), 7.65 (s, 1H), 3.93 (s, 3H); **^{13}C NMR** (101 MHz, $CDCl_3$) δ 163.2 (s), 150.9 (s), 149.9 (s), 139.2 (s), 129.1 (s), 125.1 (s), 53.3 (s); **MS** (ESI) m/z 206 [$(M + H)^+$, 100], 208 [84]; **HRMS** (ESI) m/z [M + H]$^+$ calculated for $C_7H_6Cl_2NO_2$ 205.9770, found 205.9766 (+2.9 ppm error).

Ethyl 2,5-d_2-isonicotinate S10

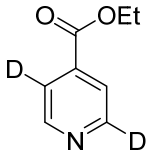

S10

To a suspension of methyl 2,5-dichloroisonicotinate (500 mg, 2.4 mmol, 1.0 eq.) and K_2CO_3 (850 mg, 6.2 mmol, 2.5 eq.) in EtOD (10 mL) in a 30 mL Parr reactor was added 5% Pd/C (50 mg, 10 wt%). The reactor was sealed, purged with N_2, then pressurised with D_2 (8 bar). The reaction mixture was stirred at room temperature for 4 hours. The pressure was released and the suspension was filtered through Celite® and washed with EtOH. The filtrate was concentrated under reduced pressure and purified by flash column chromatography with 1:1 petrol-EtOAc as eluent to give ethyl 2,5-d_2-isonicotinate **S10** (268 mg, 72%) as a colourless oil, **^{1}H NMR** (400 MHz, $CDCl_3$) δ 8.75 (s, 1H), 7.82 (s, 1H), 4.39 (q, J = 7.1 Hz, 2H), 1.39 (t, J = 7.1 Hz, 3H); **^{13}C NMR** (101 MHz, $CDCl_3$) δ 165.2 (s), 150.6 (s), 150.3 (t, J = 27.3 Hz), 137.6 (s), 122.8 (s), 122.7 (t, J = 25.6 Hz), 61.9 (s), 14.3 (s); **MS** (ESI) m/z 154 [$(M + H)^+$, 100], 126 [64]; **HRMS** (ESI) m/z [M + H]$^+$ calculated for $C_8H_8D_2NO_2$ 154.0832, found 154.0832 (–0.3 ppm error).

Methyl 2,5-d_2-isonicotinate S11

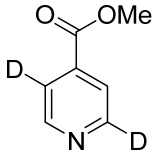

S11

A suspension of ethyl 2,5-d_2-isonicotinate (268 mg, 1.8 mmol, 1.0 eq.) and K_2CO_3 (25 mg, 0.18 mmol, 0.1 eq.) in MeOD (3 mL) was heated to 110 °C under microwave irradiation for 1 hour. The reaction mixture was concentrated under reduced pressure and purified by flash column chromatography with 2:1 petrol-EtOAc as eluent to give methyl 2,5-d_2-isonicotinate XX (124 mg, 51%) as a colourless oil; **^{1}H NMR** (400 MHz, $CDCl_3$) δ 8.74 (s, 1H), 7.80 (s, 1H), 3.92 (s, 3H); **^{13}C NMR** (101 MHz, $CDCl_3$) δ 165.6 (s), 150.6 (s), 150.3 (t, J = 27.8 Hz), 137.2 (s), 122.7 (s), 122.6 (t, J = 25.7 Hz), 52.8 (s); **MS** (ESI) *m/z* 140 [(M + H)$^+$, 100]; **HRMS** (ESI) *m/z* [M + H]$^+$ calculated for $C_7H_6D_2NO_2$ 140.0675, found 140.0680 (–3.5 ppm error).

2,5-d_2-isonicotinamide 6a

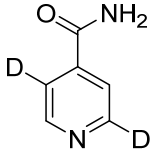

6a

A solution of methyl 2,5-d_2-isonicotinate (30 mg, 0.22 mmol, 1.0 eq.) in ammonia (5 mL, 7 N solution in methanol) was stirred at room temperature for 24 hours. The reaction mixture was concentrated and purified by flash chromatography with 1:9 MeOH-CH_2Cl_2 as eluent to give 2,5-d_2-isonicotinamide **6a** (27 mg, 100%) as a colourless solid, **^{1}H NMR** (400 MHz, CD_3OD) δ 8.69 (s, 1H), 7.82 (s, 1H), 4.97 (s, 2H); **^{13}C NMR** (101 MHz, CD_3OD) δ 169.7 (s), 150.9 (s), 150.6 (t, J = 27.9 Hz), 143.3 (s), 123.1 (s), 122.9 (t, J = 26.8 Hz); **MS** (ESI) *m/z* 125 [(M + H)$^+$, 100]; **HRMS** (ESI) *m/z* [M + H]$^+$ calculated for $C_6H_5D_2N_2O$ 125.0678, found 125.0680 (–1.1 ppm error).

2. NMR polarization transfer experiments

2.1 Polarization transfer methods

The polarization transfer experiments that are reported were conducted in either an NMR tube that was equipped with a Young's Tap (Method A) or using an automated polarizer (Method B).

Method A

Samples for these polarization transfer experiments were based on a 5 mM solution of [IrCl(COD)(IMes)] and substrate in methanol-d_4 or ethanol-d_6 (0.6 mL). The samples were degassed prior to the introduction of *para*hydrogen at the required pressure. Samples were then shaken for 10 s in the specified fringe field of an NMR spectrometer before being rapidly transported into the magnet for subsequent interrogation by NMR spectroscopy.

Method B

For the automated polarizer measurements, samples consisted of [IrCl(COD)(IMes)] and the substrate in methanol-d_4 solution (3mL). A schematic representation of the polarizer used for flow measurements is shown in Figure S1. The Mixing Chamber (MC) is housed within a tuneable copper coil (0.5 to ±150 G). The coil was situated in a magnetic field which has the components x 4.9 – 5.1 G, y 3.3 – 3.6 G and z 1.5 – 2.1 G. All magnitudes of the magnetic fields in which polarization transfer occurs (PTF) are stated without correction for this local field). The MC houses the solvent, catalyst and substrate. Liquid and gas flow is computer-controlled via the pulse program. As such, the system is entirely automated.
*Para*hydrogen is introduced into the MC first to activate the catalyst. Nitrogen gas is used to shuttle the hyperpolarized solution from the MC to the NMR probe head for measurement. The transportation time was calibrated to 2.9 s. A further delay of 0.5 s was allowed for settling of the sample prior to signal acquisition (1 s).

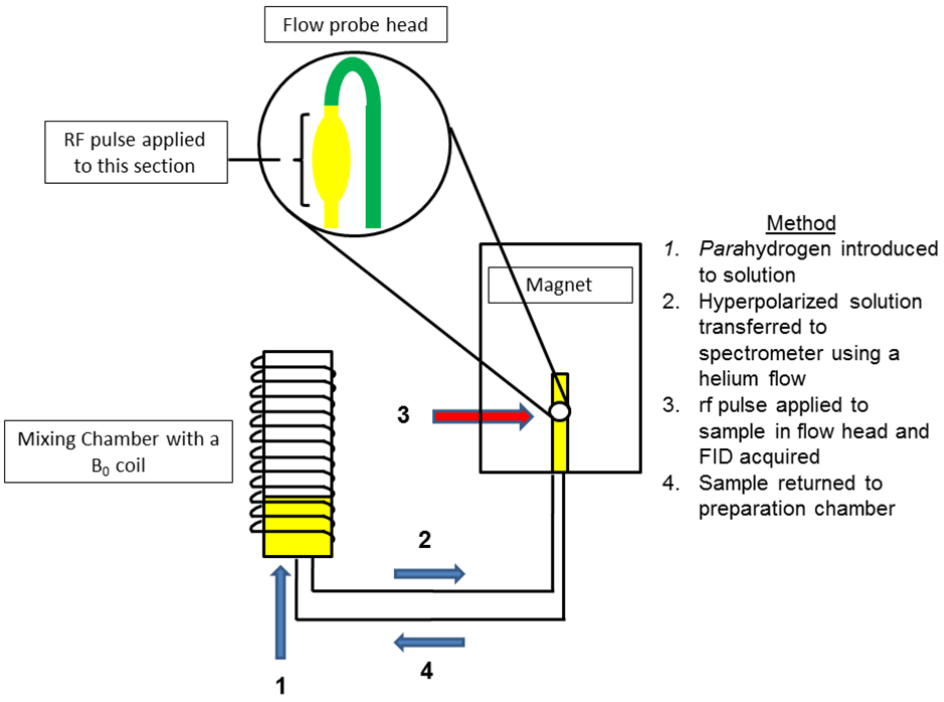

Fig. S1: Schematic representation of the polarizer, the hyperpolarization process and its subsequent NMR analysis.

2.2 ^{1}H Enhancement factors calculations and statistical analysis

For calculation of the enhancement of ^{1}H NMR signals the following formula was used:

$$\mathrm{E} = \frac{\mathrm{SI(pol)}}{\mathrm{SI(unpol)}}$$

Where, E = enhancement, SI(pol) = signal of polarized sample, SI(unpol) = signal of unpolarized (reference) sample. Experimentally, both spectra were recorded on the same sample using identical acquisition parameters, including the receiver gain. The raw integrals of the relevant resonances in the polarized and unpolarized spectra were then used to determine the enhancement levels.

Errors corresponding to the determination of the enhancement of individual sites have been calculated using the standard deviation formula

$$\varepsilon = \sqrt{\frac{\sum(x - \bar{x})^2}{n}}$$

where $\bar{x}$ is the sample mean average of the enhancements obtained after performing several experiments on the same sample and n is the number of experiments (typically between 5 and 7). The values ε obtained for each site were used in the calculation of the

errors for the total enhancement using the well-known method for the propagation of uncertainty.

2.3 Representative ^{1}H NMR spectra of the SABRE effect in deuterated agents

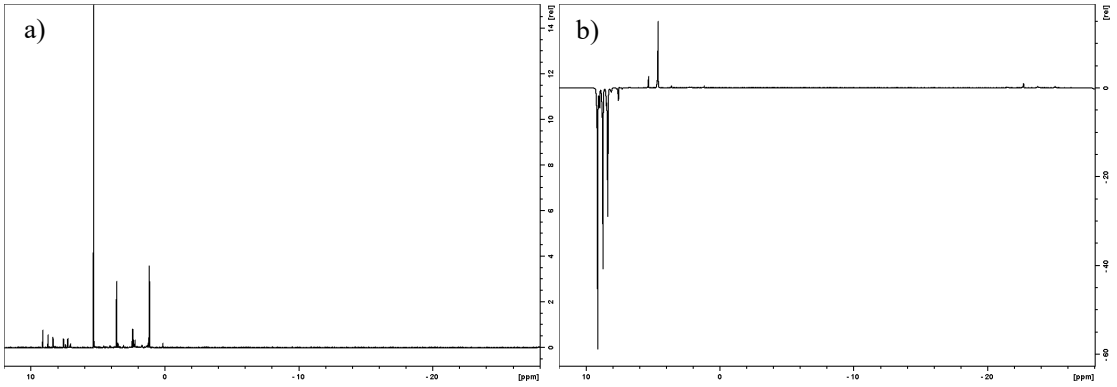

Fig. S2: l) Thermal ^{1}H NMR spectrum of [IrCl(COD)(IMes)], nicotinamide **1** under 3 bar H_2; b) ^{1}H NMR spectrum of **1** recorded after SABRE under 3 bar pH_2.

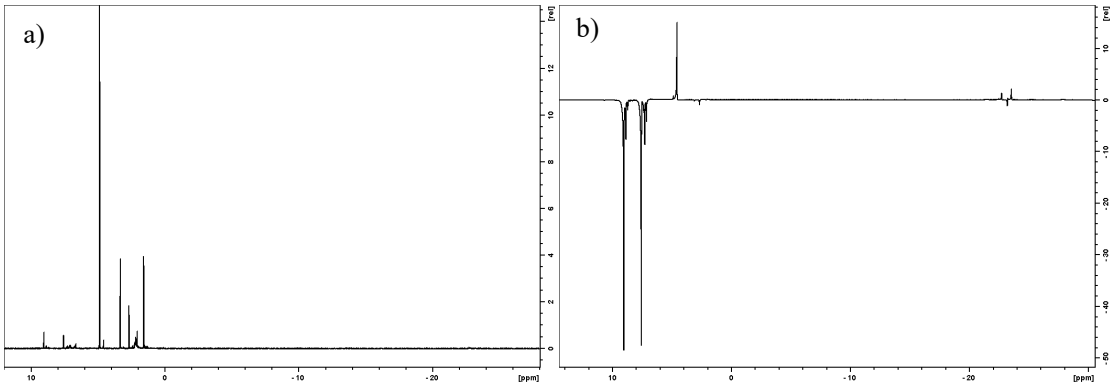

Fig. S3: a) Thermal ^{1}H NMR spectrum of [IrCl(COD)(IMes)], 4,6-d_2-nicotinamide **1f** under 3 bar H_2; b) ^{1}H NMR spectrum of **1f** recorded after SABRE under 3 bar pH_2.

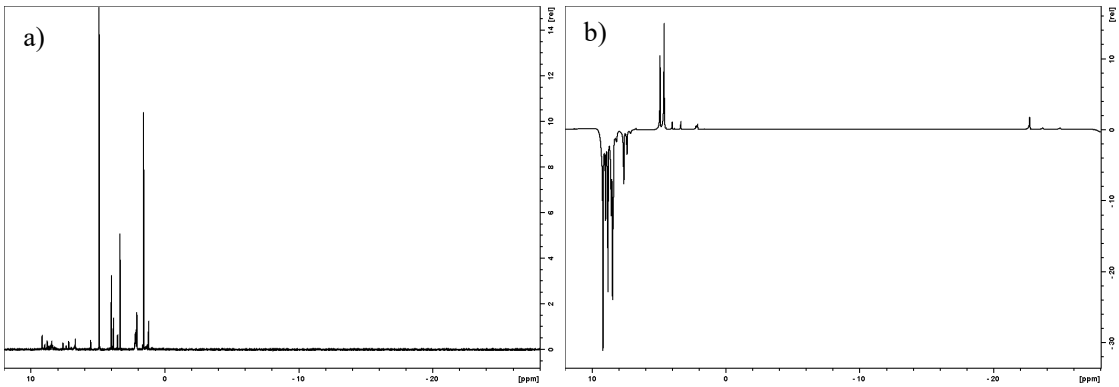

Fig. S4: a) Thermal ^{1}H NMR spectrum of [IrCl(COD)(IMes)], methyl nicotinate **2** under 3 bar H_2; b) ^{1}H NMR spectrum of **2** recorded after SABRE under 3 bar pH_2.

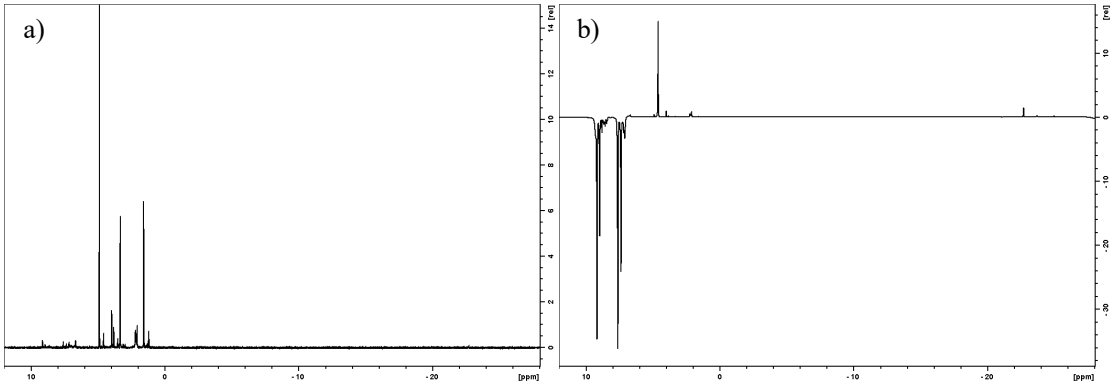

Fig. S5: a) Thermal ^{1}H NMR spectrum of [IrCl(COD)(IMes)], methyl-4,6-d$_2$-nicotinate **2b** under 3 bar H_2; b) ^{1}H NMR spectrum of **2b** recorded after SABRE under 3 bar pH_2.

2.4 Polarisation transfer results for the specified IMes catalysts

Carbene Ligand	Methanol-d_4		Ethanol-d_6	
	Site $T_{1(\text{eff., with cat.})}$ (s)	Polarization (%)	Site $T_{1(\text{eff., with cat.})}$ (s)	Polarization (%)
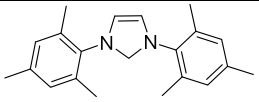 IMes	H-2 : 5.8 H-5 : 21.1	H-2: 10.9 H-5: 9.4	H-2 : 5.9 H-5 : 15.5	H-2: 7.5 H-5: 5.5
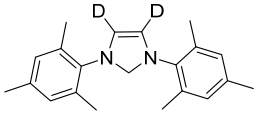 d_2-IMes	H-2 : 5.8 H-5 : 20.9	H-2: 10.1 H-5: 9.5	H-2 : 5.5 H-5 : 15.6	H-2: 9.3 H-5: 8.2
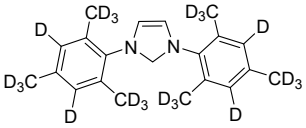 d_{22}-IMes	H-2: 7.7 H-5: 26.6	H-2: 24.1 H-5: 19.9	H-2 : 7.7 H-5 :17.2	H-2: 26.8 H-5: 16.6
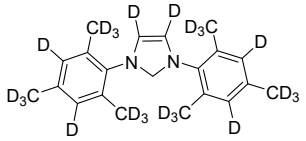 d_{24}-IMes	H-2 : 9.5 H-5 : 33.5	H-2 : 18.6 H-5 : 16.5	H-2 : 7.5 H-5 : 19.3	H-2: 13.3 H-5: 8.2

Table S1: Polarisation transfer levels and T_1 values of methyl-4,6-d2-nicotinate **2b** achieved via transfer with the specified deuterated catalysts of form [IrCl(COD)(NHC)] and 3 bar p-H_2.

2.5 Effect of *p*-H_2 pressure on polarisation transfer with [IrCl(COD)(d_{22}-IMes)]

p-H_2 Pressure (bar)	Methanol-d_4	Ethanol-d_6
	Polarization (%)	Polarization (%)
3.0	H2 : 24.1 H5 : 19.9	H2: 26.8 H5: 16.6
4.0	H2: 26.4 H5: 23.3	H2: 39.1 H5: 25.2
5.5	H2: 28.5 H5: 23.4	H2: 41.7 H5: 26.5

Table S2: Polarisation levels achieved with methyl-4,6-d2-nicotinate **2b** in conjunction with [IrCl(COD)(d_{22}-IMes)].

2.6 Use of methyl-2,4,5,6-d_4 nicotinate as a co-substrate

Methyl-2,4,5,6-d_4-nicotinate was used as a co-substrate to further reduce spin dilution in the active catalyst to achieve optimal polarisation of **2b**. A sample containing 5 mM of [IrCl(COD)(d_{22}-IMes)], 1 equivalent of **2b** and 3 equivalents of methyl-2,4,5,6-d_4-nicotinate in methanol-d_4 (0.6 mL) was prepared and exposed to increasing pressures of *p*-H_2 as shown in Table S3.

p-H_2 Pressure (bar)	Polarization (%)
3.0	H2: 40.0 H5: 35.1
4.5	H2: 46.3 H5: 39.7
5.5	H2: 49.8 H5: 39.7

Table S3: Polarisation levels achieved with [IrCl(COD)(d_{22}-IMes)], 1 eq. methyl-4,6-d2-nicotinate **2b** and 3 eq. methyl-2,4,5,6-d_4-nicotinate.

2.7 Kinetic behaviour of 2b with [IrCl(COD(NHC)] under H_2

The kinetic behaviour of **2b** with [IrCl(COD)(IMes)] and [IrCl(COD)(d_{22}-IMes)] under 3 bar H_2 was examined using exchange spectroscopy, as follows.

A series of exchange spectroscopy (EXSY) measurements were performed to probe the dynamic behaviour of these systems. This process involved the selective excitation of a single resonance and the subsequent measurement of a ^{1}H NMR spectrum at time, *t*, after the initial pulse. The resulting measurements consisted of a series of data arrays such that t is varied typically between 0.1 to 1.0 s, to encode the reaction profile. The precise values were varied with temperature to suit the speed of the process. Data was collected for a range of temperatures and sample concentrations. Integrals for the interchanging peaks in the associated ^{1}H EXSY spectra were obtained and converted into a percentage of the total detected signal.

These data were then analysed as a function of the mixing time according to a differential kinetic model [10]. Rates of exchange were determined by employing a Runge-Kutta(6, 7) scheme to solve the system of differential equations and a Levenberg–Marquardt algorithm(8, 9) to minimize the sum of the residuals in the associated least mean squares analysis. The theoretical model used to fit the experimental EXSY data involved a two-site exchange (A ↔ B), as expressed by the equations below:

$$-\frac{dA}{dt} = -K_{ab} * A + K_{ba} * B$$

$$-\frac{dB}{dt} = +K_{ab} * A - K_{ba} * B$$

An example of typical build-up/decay curves obtained from the integration of the experimental EXSY data, together with the corresponding fitted data is presented below.

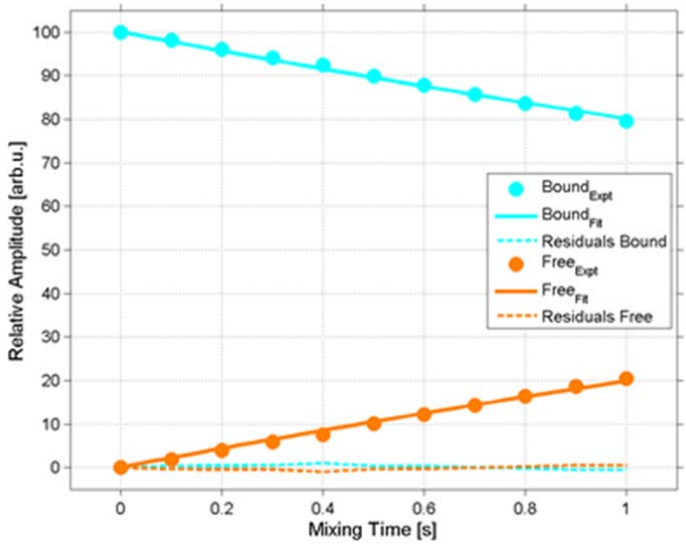

Fig. S6: Evolution of the ligand loss process as a function of time.

	[IrCl(COD)(IMes)]	[IrCl(COD)(d_{22}-IMes)]
Temperature (K)	**Rate (s^{-1})**	**Rate (s^{-1})**
298	10.0 ± 0.1	9.1 ± 0.1
293	5.1 ± 0.1	4.8 ± 0.1
283	1.3 ± 0.1	1.2 ± 0.1
273	0.3 ± 0.1	0.2 ± 0.1
263	No Exchange	No Exchange

Table S4: Rate of equatorial ligand build up in solution.

2.8 T_1 relaxation data for 2b in ethanol-d_6:D_2O solvent mixtures

The relaxation rate of **2b** in varying mixtures of ethanol-d_6:D_2O was recorded using inversion recovery at 9.4 T. These data are presented in Fig. S6.

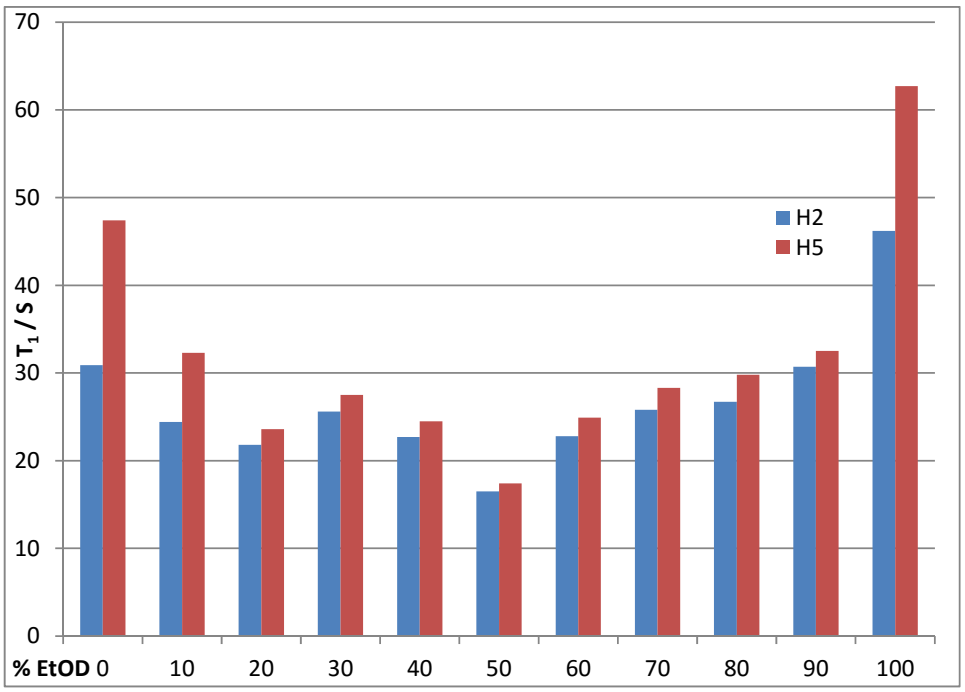

Fig. S7. T_1 relaxation data for 2b as a function of ethanol-d_6:D_2O solvent mixture composition (%).

2.9 T_1 relaxation data in H_2O solution containing 5% D_2O

The relaxation of each of the substrates was also monitored in 95% H_2O 5% D_2O solution using an inversion recovery sequence with water suppression at 9.4 T. These data are presented in Table s5.

Agent	T_1 Relaxation Time (s) (Under O_2)		Agent		T_1 Relaxation Time (s)	
1 	H-2: H-4: H-5: H-6:	5.9 4.6 4.6 5.9	**2c** 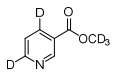		H-2: H-5:	6.5 9.7
1a 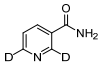	H-4: H-5:	4.2 4.6	**2d** 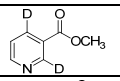		H-5: H-6:	5.7 5.0
1b 	H-5: H-6:	5.4 4.8	**2e** 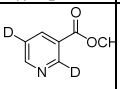		H-4: H-6:	7.4 6.6
1c 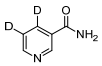	H-2: H-6:	5.0 6.3	**3** 		H-3/H-6 H-4/H-5	7.7 7.5
1d 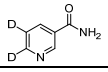	H-2: H-4:	4.8 6.2	**3a** 		H-4 H-6	9.7 9.1
1e 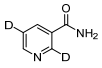	H-4: H-6:	5.4 5.6	**4** 		H-2 H-4/H-6 H-5	7.3 6.9 6.4

1f	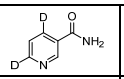	H-2: 5.6 H-5: 8.6		**4a**		H-4/H-6	8.6
1g	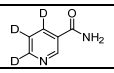	H-2: 5.8		**5**		H	7.3
2	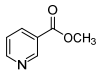	H-2: 6.0 H-4: 4.1 H-5: 4.1 H-6: 5.1		**5a**		H-3/H-6	8.5
2a	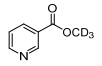	H-2: 6.9 H-4: 5.0 H-5: 4.2 H-6: 5.6		**6**		H-2/H-6 H-3/H-5	4.9 4.4
2b	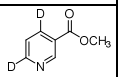	H-2: 6.6 (4.4) H-5: 9.3 (6.1)		**6a**		H-3 H-6	6.5 5.9

Table S5. T_1 relaxation times for the specified substrates in 95% H_2O 5% D_2O solution

3. SABRE MRI Collection

The SABRE experiments used the substrate and catalyst concentrations detailed below. Samples were prepared containing **1** and **2** in 3.0 ml of deuterated solvent. Arrays of measurements were collected using either 5 or 20 equivalents of substrate to 5 mM of iridium. Typical samples reflect the following situations:

i. 5 mM catalyst + 20 mM substrate (1:4 ratio) in 3.0 ml d_4-methanol (MeOD).

ii. 5 mM catalyst + 20 mM substrate (1: 4 ratio) in 3.0 ml d_6-ethanol (EtOD).

iii. 5 mM catalyst + 100 mM substrate (1: 20 ratio) in 3.0 ml d_6-ethanol (EtOD).

It should be noted that when a 100 mM loading is employed, the d_{22}-IMes catalyst yields 1.15% polarisation in **1f** and T_1 values of 13.2 and 22.1 s respectively. When **2c** is examined in the same way the T_1's change to 16.1 and 24.9 s whilst the average polarisation level becomes 2.6%. In contrast, when IMes itself is used, the corresponding T_1 values are 10.7, 21.0, 10.3 and 21.6 s whilst the enhancement levels fall to 0.9 and 1.55% respectively.

3.2 MRI Instrumentation and Procedures

3.2.1 MRI instrumentation

All images have been acquired using a 400 MHz wide-bore vertical Bruker spectrometer, equipped with a Avance III console and a Great 60 gradient unit. The maximum amplitude delivered by the microimaging gradient set was 1T/m. Detection was done using a 30 mm diameter double resonance (^{1}H-^{13}C) birdcage. Unless otherwise stated, hyperpolarisation experiments were performed with the help of an automated Bruker polariser (Method B, presented in section 2.2).(10) The measurements performed at pressures higher than 3 bar pH$_2$ were done using Method A as presented in section 2.2 and employing a 20 s polarisation transfer time.

3.2.2 MRI acquisition methods

All images presented here were recorded using a one shot spin echo based acquisition protocol (RARE(11)) with slice selective Gaussian pulses with matched bandwidths. For the experiments performed using the automated polariser image acquisition parameters were as follows: field of view (FOV) 20 x 20 mm^2, matrix size 64 x 64, slice thickness 2 mm and 5 mm (for the experiments performed in MeOD and EtOD respectively), typical acquisition time 260 ms per image. In the case of the experiments performed using a water suppression scheme, the image acquisition parameters were kept the same, except for the FOV (30 x 30 mm^2).

Solvent suppression was accomplished by using a VAPOR (variable power and optimized relaxation delays(12)) train of pulses centred on the water resonance, with a wide bandwidth, which covered not only the H_2O signal but also the signals coming from the residual protons in the deuterated solvents. The total duration of the suppression module was 660 ms.

3.2.3 MRI data processing and statistical analysis

All results were processed using Bruker software (Paravision 5.1) and home-developed post processing routines written in MATLAB. Prior to Fourier transformation, data were zero-filled once (final matrix size 128 x 128) and a sine bell squared filter was applied.

Signal-to-noise values were calculated using the ratio between the mean of the signal and the standard deviation of the noise. In most cases the values obtained for the selectively deuterated substrates are expressed as relative to the corresponding values obtained for the protio molecule.

3.3 Results

3.3.1 Image intensity optimisation through selective deuteration

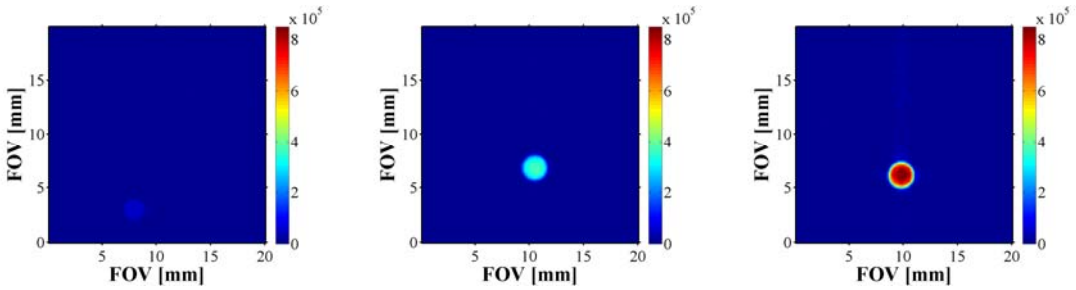

Fig. S8. Images of 20 mM hyperpolarised 1 in MeOD; 1a (left) 1d (centre) and 1f (right).

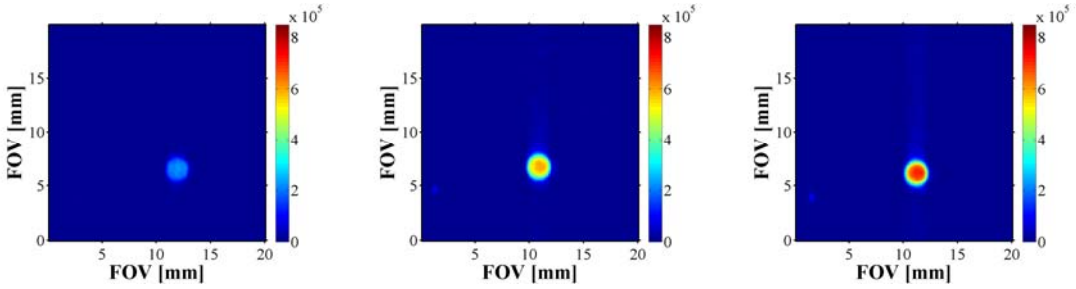

Fig. S9. Images of 20 mM hyperpolarised 2 in MeOD; 1 (left) 2b (centre) and 2c (right).

3.3.2 Effects of relaxation on image quality

In order to probe the effect of relaxation on the image intensity, a set of images of each sample was acquired in identical conditions but with variable delays before the transfer of the sample in the magnet. The purpose of this was to estimate the effective signal left after various times from the end of the polarisation process, as would be required in real life applications (delivery through an injection or catheter) in which the delivery speed needs to be adjusted according to clinical requirements. The waiting times employed were adjusted as a function of the substrate's relaxation rate and were typically between 0 and 30 s. A centric sampling of the *k*-space was employed to minimise the effect the transverse relaxation might have on the signal.

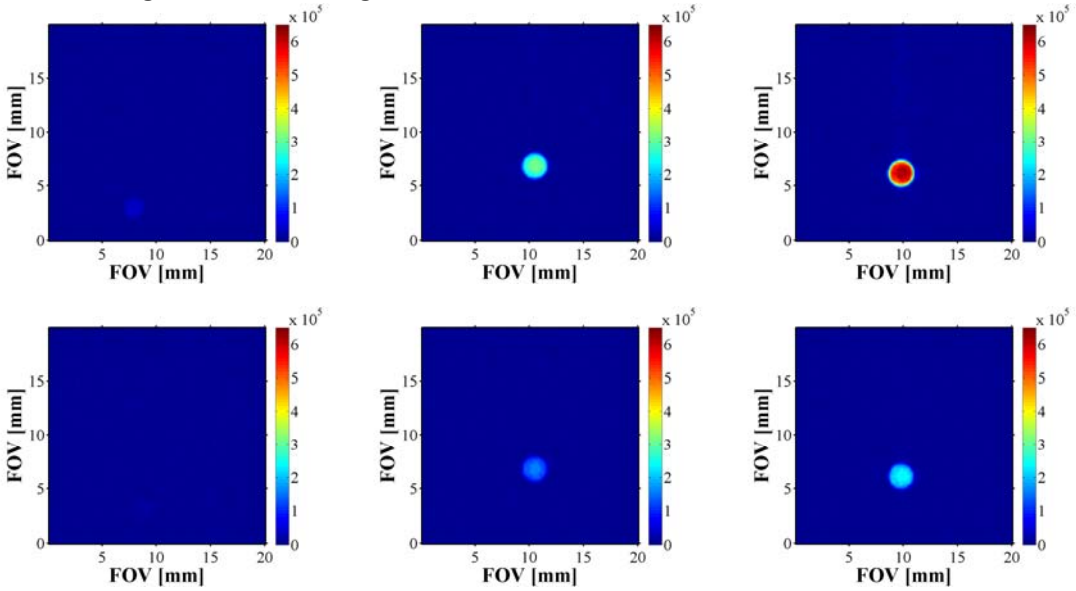

Fig. S10 Images of 20 mM hyperpolarised 1 in MeOD. **1a** (left), **1d** (centre) and **1f** (right) after 5 s (top) and 10 s (bottom) from the polarisation transfer process.

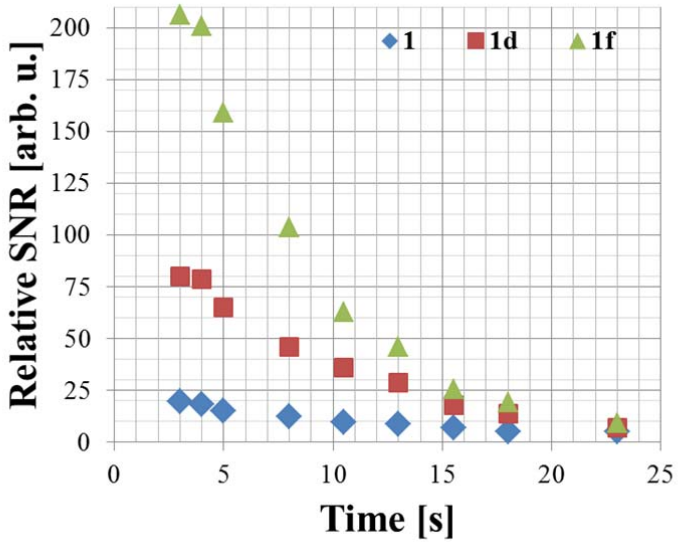

Fig. S11 SNR decay as a function of the delay between the polarisation transfer process and image acquisition for 1.

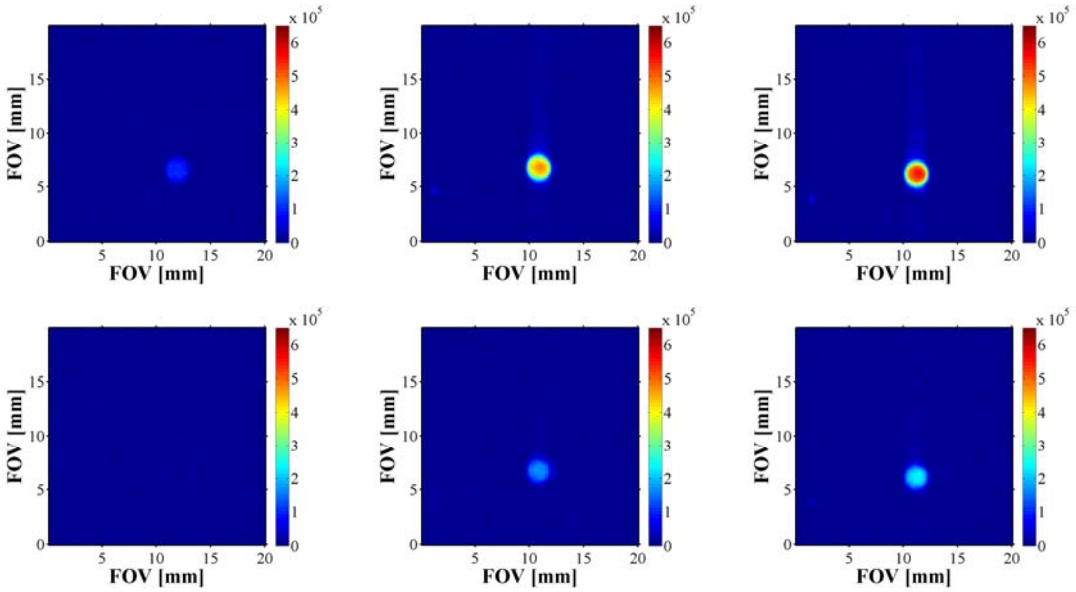

Fig. S12 Images of 20 mM hyperpolarised 2 in MeOD. **2** (left), **2b** (centre) and **2c** (right) after 5 s (top) and 10 s (bottom) from the polarisation transfer process.

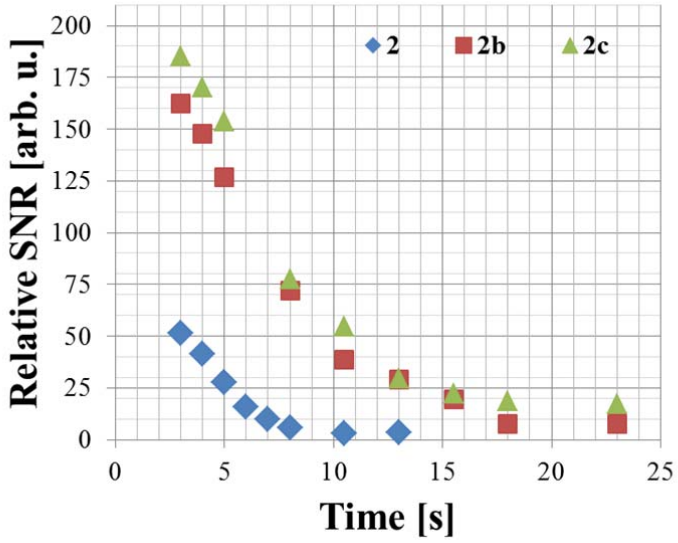

Fig. S13 SNR decay as a function of the delay between the polarisation transfer process and image acquisition for **2**, **2b** and **2c**.

3.3.3 Image contrast optimisation by water and solvent suppression

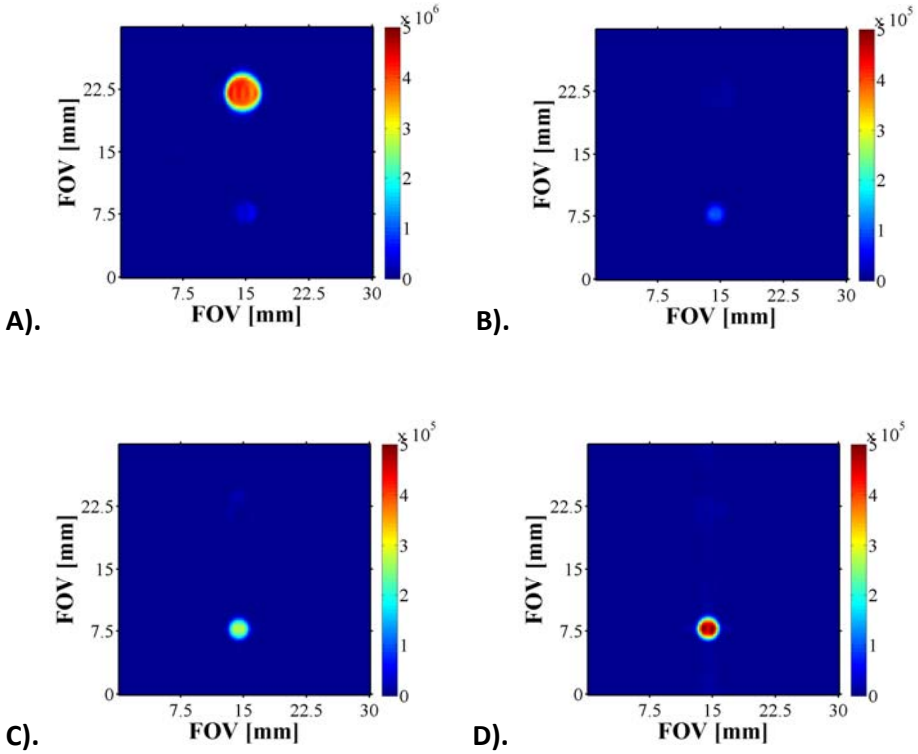

Fig. S14 Images of a 5 mm water tube and 100 mM hyperpolarised substrate in EtOD**.** A). no water suppression, hyperpolarised **1**, B). water suppression on, hyperpolarised **1**, C). water suppression on, hyperpolarised **1f** and D). water suppression on, hyperpolarised **2b**.

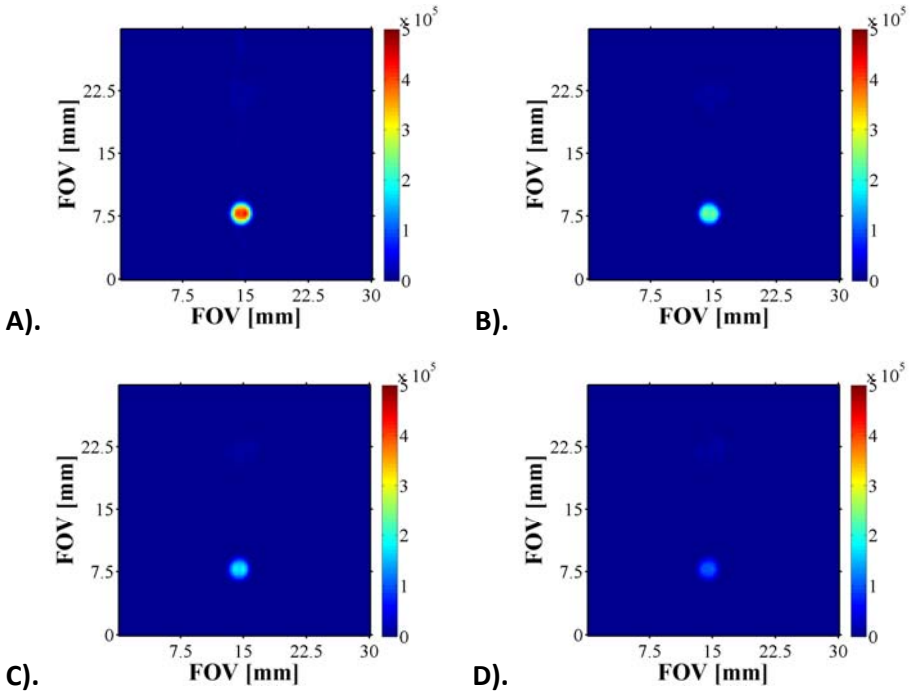

Fig. S15 Images of a 5 mm water tube and 100 mM 2b in EtOD**.** The images were acquired using a water suppression scheme A). 10 s, B). 15 s, C). 20 s and D). 30 s after the polarisation transfer process.

3.3.4 Effects of pH$_2$ pressure on image quality

The effects of pH_2 pressure on image intensity and contrast were tested using a pressure resistant tube and the substrates 1f and 2b. The results are presented below.

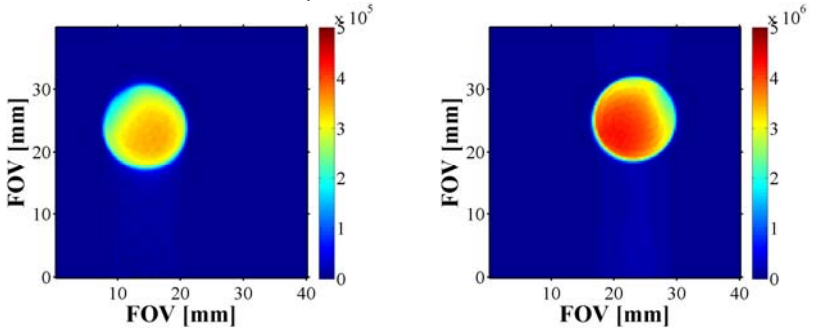

Fig. S16 Images of hyperpolarised **1f**. The images were acquired using 3 bar pH_2 pressure (left) and 8 bar of pH_2 pressure (right) in MeOD. SNR: 348 and 3847 respectively.

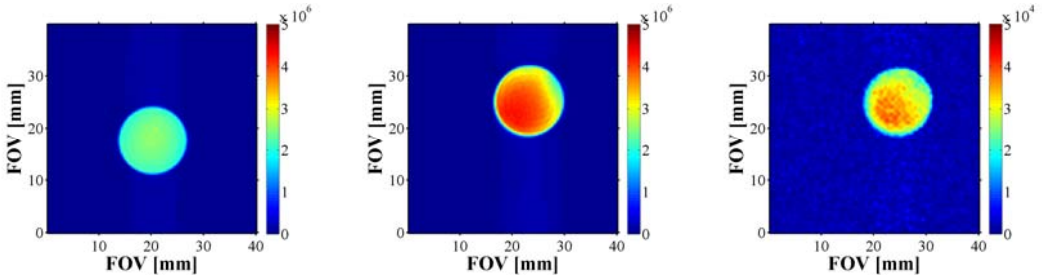

Fig. S17 Images of water (left), hyperpolarised **1f** (centre) and **1f** in Boltzmann equilibrium conditions. Catalyst:Substrate ratio 1:20. SNR: 2384, 3847 and 35 respectively.

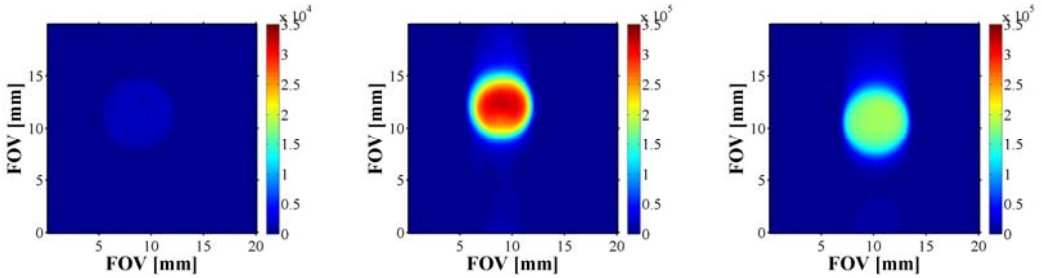

Fig. S18 Images of hyperpolarised 2b. The images were acquired under Boltzmann equilibrium conditions (left), hyperpolarised in MeOD (centre) and hyperpolarised in EtOD (right). Catalyst:Substrate ratio 1:4. SNR: 9, 1482, 939.

References

1. Khoje AD & Gundersen L-L (2011) Reactivity and regioselectivity in Stille couplings of 3-substituted 2,4-dichloropyridines. *Tetrahedron Lett.* 52(4):523-525.
2. Wallace EM*, et al.* (2005) Potent and Selective Mitogen-Activated Protein Kinase Kinase (MEK) 1,2 Inhibitors. 1. 4-(4-Bromo-2-fluorophenylamino)-1- methylpyridin-2(1H)-ones. *J. Med. Chem.* 49(2):441-444.
3. Vazquez-Serrano LD, Owens BT, & Buriak JM (2006) The search for new hydrogenation catalyst motifs based on N-heterocyclic carbene ligands. *Inorg. Chim. Acta* 359(9):2786-2797.
4. Leitao EM, Dubberley SR, Piers WE, Wu Q, & McDonald R (2008) Thermal Decomposition Modes for Four-Coordinate Ruthenium Phosphonium Alkylidene Olefin Metathesis Catalysts. *Chemistry – A European Journal* 14(36):11565-11572.
5. Fekete M*, et al.* (2013) Iridium(III) Hydrido N-Heterocyclic Carbene–Phosphine Complexes as Catalysts in Magnetization Transfer Reactions. *Inorg. Chem.* 52(23):13453-13461.
6. Kutta W (1901) Beitrag zur näherungsweisen Integration totaler Differentialgleichungen. *Z.Math.Phys.* 46:435-453.
7. Runge C (1895) Ueber die numerische Auflösung von Differentialgleichungen. *Mathematische Annalen* 46(2):167-178.
8. Levenberg K (1944) A Method for the Solution of Certain Non-Linear Problems in Least Squares. *The Quarterly of Applied Mathematics* (2):164-168.
9. Marquardt D (1963) An Algorithm for Least-Squares Estimation of Nonlinear Parameters. *Journal of the Society for Industrial and Applied Mathematics* 11(2):431-441.
10. Mewis RE*, et al.* (2014) Probing signal amplification by reversible exchange using an NMR flow system. *Magn. Reson. Chem.* 52(7):358-369.
11. Hennig J, Nauerth A, & Friedburg H (1986) RARE imaging: A fast imaging method for clinical MR. *Magnetic Resonance in Medicine* 3(6):823-833.
12. Griffey RH & P. Flamig D (1969) VAPOR for solvent-suppressed, short-echo, volume-localized proton spectroscopy. *Journal of Magnetic Resonance (1969)* 88(1):161-166.